


RESEARCH ARTICLE

Open Access



Chromatin modifier *developmental pluripotency associated factor 4 (DPPA4)* is a candidate gene for alcohol-induced developmental disorders

P. Auvinen¹, J. Vehviläinen¹, H. Marjonen¹, V. Modhukur^{2,3}, J. Sokka⁴, E. Wallén¹, K. Rämö¹, L. Ahola¹, A. Salumets^{2,3,5}, T. Otonkoski^{4,6}, H. Skottman⁷, M. Ollikainen⁸, R. Trokovic⁴, H. Kahila⁹ and N. Kaminen-Ahola^{1*} 

Abstract

Background: Prenatal alcohol exposure (PAE) affects embryonic development, causing a variable fetal alcohol spectrum disorder (FASD) phenotype with neuronal disorders and birth defects. We hypothesize that early alcohol-induced epigenetic changes disrupt the accurate developmental programming of embryo and consequently cause the complex phenotype of developmental disorders. To explore the etiology of FASD, we collected unique biological samples of 80 severely alcohol-exposed and 100 control newborns at birth.

Methods: We performed genome-wide DNA methylation (DNAm) and gene expression analyses of placentas by using microarrays (EPIC, Illumina) and mRNA sequencing, respectively. To test the manifestation of observed PAE-associated DNAm changes in embryonic tissues as well as potential biomarkers for PAE, we examined if the changes can be detected also in white blood cells or buccal epithelial cells of the same newborns by EpiTYPER. To explore the early effects of alcohol on extraembryonic placental tissue, we selected 27 newborns whose mothers had consumed alcohol up to gestational week 7 at maximum to the separate analyses. Furthermore, to explore the effects of early alcohol exposure on embryonic cells, human embryonic stem cells (hESCs) as well as hESCs during differentiation into endodermal, mesodermal, and ectodermal cells were exposed to alcohol in vitro.

Results: *DPPA4*, *FOXP2*, and *TACR3* with significantly decreased DNAm were discovered—particularly the regulatory region of *DPPA4* in the early alcohol-exposed placentas. When hESCs were exposed to alcohol in vitro, significantly altered regulation of *DPPA2*, a closely linked heterodimer of *DPPA4*, was observed. While the regulatory region of *DPPA4* was unmethylated in both control and alcohol-exposed hESCs, alcohol-induced decreased DNAm similar to placenta was seen in in vitro differentiated mesodermal and ectodermal cells. Furthermore, common genes with alcohol-associated DNAm changes in placenta and hESCs were linked exclusively to the neurodevelopmental pathways in the enrichment analysis, which emphasizes the value of placental tissue when analyzing the effects of prenatal environment on human development.

*Correspondence: nina.kaminen@helsinki.fi

¹ Environmental Epigenetics Laboratory, Department of Medical and Clinical Genetics, Medicum, University of Helsinki, 00290 Helsinki, Finland
Full list of author information is available at the end of the article



© The Author(s) 2022. **Open Access** This article is licensed under a Creative Commons Attribution 4.0 International License, which permits use, sharing, adaptation, distribution and reproduction in any medium or format, as long as you give appropriate credit to the original author(s) and the source, provide a link to the Creative Commons licence, and indicate if changes were made. The images or other third party material in this article are included in the article's Creative Commons licence, unless indicated otherwise in a credit line to the material. If material is not included in the article's Creative Commons licence and your intended use is not permitted by statutory regulation or exceeds the permitted use, you will need to obtain permission directly from the copyright holder. To view a copy of this licence, visit <http://creativecommons.org/licenses/by/4.0/>. The Creative Commons Public Domain Dedication waiver (<http://creativecommons.org/publicdomain/zero/1.0/>) applies to the data made available in this article, unless otherwise stated in a credit line to the data.

Conclusions: Our study shows the effects of early alcohol exposure on human embryonic and extraembryonic cells, introduces candidate genes for alcohol-induced developmental disorders, and reveals potential biomarkers for prenatal alcohol exposure.

Keywords: Prenatal alcohol exposure, PAE, FASD, DNA methylation, Gene expression, Placenta, Human embryonic stem cells, Germ layers, Endoderm, Mesoderm, Ectoderm, Environmental epigenetics, Embryonic development, *DPPA4*, *DPPA2*, *FOXP2*, *TACR3*

Background

Prenatal alcohol exposure (PAE) is associated with a broad spectrum of permanent structural, physiological, neurocognitive, and behavioral disorders of the exposed, often growth-restricted offspring [1]. Fetal alcohol spectrum disorders (FASD) are a consequence of PAE and an umbrella term for all alcohol-induced developmental disorders. PAE is one of the most harmful environmental factors affecting permanently 3–5% of individuals in the Western world [2].

Several lines of evidence suggest that the epigenome of developing embryo is sensitive to environmental effects in the early pregnancy, during the dynamic period of epigenetic reprogramming [3, 4]. Alcohol-induced epigenetic alterations have been observed in the offspring of our early PAE mouse model [5, 6] as well as human and mouse embryonic stem cells [7, 8]. Those early epigenetic changes could affect gene regulation and consequently developmental programming. Depending on the function of the cell or tissue types, they could contribute to the complex phenotype of FASD.

To explore the etiology of FASD, we have collected placental samples from PAE and control newborns at birth. Placenta is an accessible human tissue and a promising implement for identifying the effects of intrauterine environment on embryonic development, including neuronal development [9, 10]. Here, by performing genome-wide DNA methylation (DNAm) analysis of placenta, we discovered a candidate gene *developmental pluripotency associated factor 4* (*DPPA4*), which was hypomethylated particularly in the early alcohol-exposed placentas. *DPPA4* functions as a heterodimer with *developmental pluripotency associated factor 2* (*DPPA2*) and both proteins are required for efficient binding and chromatin remodeling [11]. By modifying chromatin structure, these epigenetic priming factors facilitate transition between pluripotency and differentiation [11–13], which makes them plausible candidate genes for developmental disorders. Both genes are located in tandem on chromosome 3q13.13, they are regulated by promoter DNAm in mouse, and are expressed for a short time in the beginning of embryonic development [14]. To explore the effects of early alcohol exposure on human embryonic cells, and more specifically on the regulation of *DPPA2*

and *DPPA4*, we performed genome-wide DNAm and gene expression analyses for in vitro alcohol-exposed human embryonic stem cells (hESCs). Furthermore, hESCs were in vitro alcohol-exposed during differentiation into the endodermal, mesodermal, and ectodermal cells.

Alcohol-induced epigenetic changes in the first embryonic cells could be fixed in persistent cellular memory and mitotically transmitted to different cell and tissue types. Indeed, variety of PAE-associated DNAm changes in peripheral blood [15] and buccal epithelial cells (BECs) [16, 17] of children with FASD have been observed in previous genome-wide studies. Therefore, we examined whether PAE-associated epigenetic alterations can be detected not only in the extraembryonic placenta, but also in embryonic white blood cells (WBCs) from cord blood or BECs of the same newborns. Those changes could be the first fingerprints of PAE, potential future biomarkers for FASD, which would enable early diagnosis and personalized support for the development of the affected children.

Methods

Epigenetics of FASD (epiFASD) cohort

Women ($n = 80$) with substantial alcohol consumption were recruited to this study in a special outpatient clinic for pregnant women with substance use problems in Helsinki University Hospital, Finland during the years 2013–2020 (Table 1 and Additional file 1: Table S1). The timing of maternal alcohol consumption was registered using self-reported information. To avoid specific individual level data, the timing of consumption is presented in three categories according to pregnancy trimesters (Additional file 1: Table S1 and Additional file 2: Fig. S1). The amount of maternal alcohol consumption was registered using self-reported information: Alcohol Use Disorders Identification Test (AUDIT) or the number of alcohol units consumed per week (ad) (one unit is 12 g of ethyl alcohol). A 10-item screening tool AUDIT, developed by the World Health Organization, estimates alcohol consumption, drinking behavior, and alcohol-related problems [18]. Maternal alcohol consumption is presented in three categories according to AUDIT scores or ad [19, 20]. However, self-reported information (not

Table 1 General characteristics of PAE and control newborns as well as their mothers included in the phenotype analysis

Newborns	Sex (male/female)	Gestational age (weeks +days)	Birth weight (g)	Birth length (cm)		HC (cm)	Placental weight (g)
				SD	SD		
Control (n = 100) mean (±SD)	52.0/ 48.0%	all 40 +3 (±1 +0)	3661 (±366)	0.07 (±0.9)	51 (±2)	35.5 (±1.3)	626.5 (±126.4)
PAE (n = 80) mean (±SD)	42.5/57.5%	39 +4 (±1 +5)	3327 (±554)	-0.23 (±0.1)	49 (±3)	34.4 (±1.9)	596.6 (±136.7)
Difference between groups, P-value	0.231 ⁽³⁾	<.001 ⁽¹⁾	<.001 ⁽¹⁾	0.030 ⁽¹⁾	<.000 ⁽¹⁾	<.000 ⁽¹⁾	0.083 ⁽¹⁾
Early PAE (n = 27) mean (±SD)	44.4/55.6%	40 +1 (±1 +5)	3526 (±440)	-0.06 (±0.8)	50 (±2)	34.5 (±1.7)	620.7 (±160.1)
Difference between groups, P-value	0.522 ⁽³⁾	0.804 ⁽¹⁾	0.147 ⁽²⁾	0.485 ⁽²⁾	0.267 ⁽¹⁾	<.001 ⁽¹⁾	0.843 ⁽¹⁾
Mothers	AUDIT score	Alcohol consumption (ad)	Smoking (smokers/non-smokers)	Age (years)	Parity	Pre-pregnancy BMI (kg/m ²)	Gestational weight gain (kg)
Control (n = 100) mean (±SD)	18.5 (±8.4)	24.8 (18.7)	0.0/100%	31.6 (±4.6)	0.55 (±0.7)	22.8 (±3.5)	15.1 (±3.8)
PAE (n = 80) mean (±SD)	n = 44	n = 26	82.5/17.5%	29.5 (±6.8)	0.66 (±1.3)	25.4 (±5.9)	12.4 (±6.7)
Difference between groups, P-value				0.017 ⁽¹⁾	0.269 ⁽¹⁾	0.008 ⁽¹⁾	0.008 ⁽²⁾
Early PAE (n = 27) mean (±SD)	19.9 (±7.2)	31.5 (15.8)	74.1/25.9%	27.1 (±5.9)	0.26 (±0.7)	24.3 (±4.9)	15.7 (±6.9)
Difference between groups, P-value	n = 18	n = 8		0.001 ⁽²⁾	0.017 ⁽¹⁾	0.212 ⁽¹⁾	0.711 ⁽²⁾

Differences in weight, length, and head circumference (HC) of the newborns were calculated using both anthropometric measures and the standard deviations (SDs) of measures based on international growth standards adjusted for gestational age at birth and gender. Data presented as mean ±SD. P-values for PAE and control newborns as well as for early PAE and control newborns were calculated using Mann-Whitney U test (1) or two-tailed Student's t test (2) and for the proportion of males and females between the groups using Pearson chi-square (3). Differences in gestational age were calculated for all newborns and for newborns delivered spontaneously without cesarean section (CS) and induction of labor (IL). ILs due to prolonged control pregnancies (42+1) were not excluded. AUDIT: alcohol use disorders identification test before pregnancy and ad: alcohol units consumed per week

categories) about timing of drinking, AUDIT scores, and ad were used in statistical analyses. The mothers who consumed alcohol up to gestational week (GW) 7 at maximum were selected in the early PAE subgroup. Only samples with the most specified information about the maternal alcohol consumption were included (27 newborns) (Additional file 1: Table S1). According to the chart reviews, the majority, 66 (82.5%) mothers of all PAE newborns smoked, and 18 (22.5%) mothers used antidepressants or antipsychotic medication during the pregnancy. Five (6.3%) mothers used gestational diabetes mellitus medication. Four mothers had thyroid diseases, two had antihypertensive medication, and one had preventive medication for herpes. One mother had FAS diagnosis. One mother was an occasional user of stimulants and one of cannabis. Fifteen (18.8%) of the deliveries were cesarean sections (CS). Due to the preterm premature rupture of membranes, two newborns were preterm. One of the PAE newborns had two thumbs in one hand, and three had cleft lip. One newborn was Asian, one was Caucasian (other than Finnish), and two were of African origin. One's mother was Caucasian (other than Finnish), and one had African origin father. Other newborns were children of Finnish, Caucasian parents.

The control samples ($n = 100$), collected during the years 2013–2015 in Helsinki University Hospital, Finland, were from newborns of healthy Finnish, Caucasian mothers who did not use alcohol or smoke during pregnancy according to their self-reported information (Additional file 1: Table S2). Ten (10%) of the deliveries were CSs.

The information about the samples included in the early PAE subgroup as well as in each analysis is shown in the Additional file 1: Tables S1 and S2, and the general characteristics of the participants in each analysis are shown in the Additional file 1: Table S3.

Sample collection

Biological samples (placental biopsies, WBCs from umbilical cord blood, and BECs) of newborns were collected immediately after delivery. When this was not possible, placenta was stored in the fridge for a maximum of 12 h and only DNA was extracted for further analyses. The placental biopsies (1 cm³) were collected from the fetal side of the placenta within a radius of 2–4 cm from the umbilical cord, rinsed in cold 1× PBS, and stored in RNeasy[®] (Thermo Fisher Scientific) at –80 °C. WBCs were extracted from umbilical cord blood as soon as possible, at latest 16 h after birth as described previously [21]. BEC samples were collected by rubbing buccal swabs (SK-3S, Isohelix or Catch-All[™] Sample Collection Swab, Epicentre Biotechnologies) 20 times firmly against the inside of the newborn's cheek and stored at –80 °C.

Birth weight (g), birth length (cm), and head circumference (HC) (cm) were examined using international growth standards, the Fenton Preterm Growth Chart by PediTools [22], in which the gestational age at birth and sex are considered when calculating the standard deviation (z -score) of birth measures (SD of birth measures) [23].

hESC and differentiation experiments

hESC culture and alcohol treatment

Alcohol concentration of 70 mM, which corresponds to the blood alcohol concentration of a heavy drinker [24], was chosen according to a previous publication [25]. hESC lines H1 (WA01, male) and Regea08/017 (female) were cultured in E8 or in E8 Flex Medium (Gibco) on Matrigel (Corning) coated plates at 37 °C and 5% CO₂. Culture media was routinely replaced every day (every second or third day in the case of E8 Flex Medium), and cells were passaged using 0.5 mM EDTA. For the alcohol treatment, the medium was supplemented with alcohol (≥ 99.5 p-% ethanol) at a final concentration of 70 mM 48 h before the cells reached confluency and were cross-linked for chromatin immunoprecipitation (ChIP) or collected for DNA and RNA extractions. Due to alcohol evaporation, the culture media with alcohol were replaced after treatment of 24 h.

Germ layer cell differentiation and alcohol treatment

H1 cells cultured in E8 Medium on Matrigel plates were differentiated into the endodermal, mesodermal, and ectodermal cells by using the STEMdiff[™] Trilineage Differentiation Kit (StemCell Technologies, Inc.). Cells were seeded on a Matrigel-coated 6-well plates at 250,000 cells/well for the mesoderm, 1 million cells/well for the endoderm, and 1.5 million cells/well for the ectoderm, and differentiated according to the manufacturer's instructions. The cells were supplemented with 10 μ M Y-27632 for the first 24 h after seeding, and the mediums were changed daily. For the alcohol-exposed wells, the medium was supplemented with alcohol at a final concentration of 70 mM. After 5 or 7 days, the cells were collected for DNA and RNA extractions. The differentiation was confirmed by 3'mRNA sequencing (mRNA-seq) analysis, and expression profiles of gene characteristic for specific germ layers were analyzed (Additional file 2: Fig. 2).

DNA and RNA extractions

Placental genomic DNA was extracted from one to four (3.7 on average) pieces of placental tissue samples using commercial QIAamp Fast DNA Tissue Kit (Qiagen) or standard phenol-chloroform protocol. WBC DNA was extracted using QIAamp Fast DNA Tissue Kit or AllPrep

DNA/RNA/miRNA Universal Kit (Qiagen) and BEC DNA using BuccalPrep Plus DNA Isolation Kit (Isohelix). Placental RNA was extracted from the same pieces as DNA (2.9 on average) by AllPrep DNA/RNA/miRNA Universal Kit, and the same kit was used for DNA and RNA extraction from hESCs and differentiated hESCs. RNA quality was assessed using an Agilent 2100 Bioanalyzer (Agilent Technologies, Inc.), which was provided by the Biomedicum Functional Genomics Unit (FuGU) at the Helsinki Institute of Life Science and Biocenter Finland at the University of Helsinki.

DNAm microarrays

Genomic DNA (1000 ng) from available placental (all PAE $n = 69$, early PAE $n = 27$, and control $n = 66$), hESC (H1 and Regea08/017: $n = 4$ /condition, respectively), and differentiated H1 hESC (each germ layer: $n = 4$ /condition) samples was sodium bisulfite-converted using the Zymo EZ DNAm™ kit (Zymo Research), and genome-wide DNAm was assessed with Infinium Methylation EPIC BeadChip Kit (Illumina) following a standard protocol.

Genome-wide DNAm analysis

The raw DNAm dataset was pre-processed, quality controlled, and filtered using ChAMP R package [26] with default settings. The detection P -value cutoff was set at $P = 0.01$, and probe bead count > 3 in at least 95% of samples. All probes and samples passed these QC thresholds and were included in the subsequent steps. The data filtering steps included the removal of probes located in sex chromosomes and probes binding to polymorphic and off-target sites [27]. Finally, Type-I and Type-II probes were normalized using the BMIQ method. For placental samples, probes located in Finnish-specific SNPs (SNPs which overlap with any known SNPs with global minor allele frequency (MAF) and MAF in a Finnish population $> 1\%$) were removed as described previously [28]. Population-specific masking and SNP information was obtained from Zhou et al. [29]. Subsequently, a total of 588,781 probes of placental and 800,002 probes of hESC samples were retained for further downstream analysis. Potential batch effects caused by technical factors and biological covariates were studied from *singular value decomposition (SVD) plots*. For placental samples, the correction for batch effect was performed by the Empirical Bayes method using the R package ComBat [30]. Genome-wide DNAm analysis by using M -values was performed by R package Limma [31], and the model for placental samples was adjusted to consider biological covariates sex and smoking. The λ values and Quantile-Quantile (Q-Q) plots are shown in Additional file 2: Fig. S3a. Planet R package [32] was used to count placental

cell-type fractions by CIBERSORT method and used as an adjusting factor in the model. For hESCs, a mixed linear model was built by using humanzee R package [33] to remove sample-specific random effect and to adjust cell line. β -values were used for visualization and interpretation of the results and to construct the DNAm profiles of differentiated cells.

CpGs were considered as significant (hereafter differentially methylated positions, DMPs) when DNAm difference was greater than 5% ($\Delta\beta \leq -0.05$ and $\Delta\beta \geq 0.05$) and false discovery rate (FDR)-corrected P -value smaller than 0.05. Benjamini-Hochberg procedure was used to control for FDR. Annotation information of the University of California, Santa Cruz (UCSC) database about CpG sites were obtained and merged to corresponding CpG sites from IlluminaHumanMethylationEPICanno.ilm10b4.hg19 R package [34], which is based on the file “MethylationEPIC_v1-0_B4.csv” from Illumina [35]. If the UCSC database location information was missing, DMP was marked as “unknown.” In the case of multiple location entries, group “others” was used. Otherwise, the following abbreviations were used: TSS1500: 1500 bp upstream of transcription start site, TSS200: 200 bp upstream of TSS, UTR: untranslated region, N_shelf: north shelf, N_shore: north shore, S_shore: south shore, S_shelf: south shelf.

Sensitivity analysis for DMPs

To test the sensitivity of DMPs, only non-smoking samples (66 controls and 11 PAE) were selected to the differential DNAm analysis, which was adjusted only for sex. The sensitivity analysis was also performed for the samples of early PAE subgroup (66 controls and six PAE).

Sensitivity analysis for candidate genes

Samples (66 control and eight PAE) for the sensitivity analysis of three candidate genes (*DPPA4*, *FOXP2*, and *TACR3*) were selected by excluding the effects of smoking and extraction methods. The differential DNAm analysis was adjusted for sex, maternal age, mode of delivery, and parity as covariates according to the SVD plot (Additional file 2: Fig. S4a). After these adjustments, the group (control/PAE) was the most significant factor in the SVD plot, whereas other factors (AUDIT, HC, birth weight, birth length) associated with PAE and therefore cannot be adjusted for. The sensitivity analysis was also performed for the samples in the early PAE subgroup (66 controls and four PAE) (Additional file 2: Fig. S4b). The λ values of the sensitivity analyses were improved compared to DMP analyses, as expected (Additional file 2: Fig. S3b).

Differentially methylated region (DMR) analysis

DMRcate R package was used for analyzing DMRs [36]. The method uses minimum description length for detecting region boundaries in DMR identification. DMRcate was adjusted to determine probes (≥ 3) in a region with maximal allowed genomic distance of 1000 bp containing at least one CpG with $\Delta\beta \leq -0.05$ or $\Delta\beta \geq 0.05$. Further, FDR < 0.05 was defined to describe the DMR with significance.

Enrichment analysis of DMPs at genomic locations

Enrichment of DMPs at different genomic locations relative to gene (TSS1500, TSS200, 5'UTR, 1stExon, Body, 3'UTR, Others, Unknown) and relative to CpG island (N_Shelf, N_Shore, Island, S_Shore, S_Shelf, OpenSea) were calculated for both placenta and hESCs and results were compared to the proportions of probes in the EPIC Array by Fisher's exact test of homogeneity followed by pairwise comparison post hoc test.

Genome-wide average DNAm (GWAM)

After quality filtering steps, remaining 588,781 probes were used to calculate the genome-wide average DNAm levels of placental samples, and 800,002 probes were used for GWAM [37] of hESCs.

Global DNAm

Filtered and corrected DNAm data was used to predict DNAm in Alu, LINE1, and LTR using Random Forest-based algorithm implemented by REMP R package [38] as a proxy for global DNAm level. Less reliable predicted results were trimmed according to quality score threshold 1.7 and missing rate 0.2 (20%).

Pathway analysis

Enrichment analysis was performed for significant DMPs by *gometh* function in missMethyl R package [39], which considers the different number of probes per gene present on the EPIC array and CpGs that are annotated to multiple genes. missMethyl was set to use the Gene Ontology (GO) knowledgebase as the source for identifying significantly enriched biological process (BP) terms from genes which contained at least one significant DMP. Pathway analysis was also performed for significant DMRs by *goregion* function in missMethyl R package and GO:BP knowledgebase was used as a source. For the enrichment analysis, DMRs with two CpG sites were also included. None of the GO terms

were significant after FDR correction and therefore the terms with the nominal P -value < 0.05 were reported.

EpiTYPER

To validate and replicate the findings from the EPIC microarrays, DNAm profiles of target genes (*DPPA4*, *FOXP2*, and *TACR3*) were measured by MassARRAY EpiTYPER (Agena Bioscience, Inc.) in placental tissue, WBCs, BECs, and hESCs. Samples of 16 PAE and 14 control newborns were chosen for the *DPPA4* target gene and 10 PAE and 9 control newborns for other target genes. In hESCs, two biological replicates of alcohol-exposed and control cells of both H1 and Regea08/017 cell lines were used for the analysis. First, genomic DNA (500–1000 ng) was subjected to sodium bisulfite conversion using EZ-96 DNA Methylation™ kit (Zymo Research). PCR amplification was performed in three independent 10 or 15 μ l reactions using HotStar PCR kit (Qiagen) following the provider's instructions. Primers for the target regions were designed using EpiDesigner software [40] incorporating CpGs chosen for each target according to the microarray analysis. Primers for *TACR3* DMP cg18538958 with the largest effect size were unable to design and therefore a correlating probe cg16461251 ($r = 0.973$, $P < 0.001$, $n = 136$, Spearman's rank correlation) was selected for the analysis. Primers and PCR protocols for each target sequence are presented in Additional file 1: Tables S4 and S5. Owing to the proximity of two CpGs in one unit in *FOXP2*, they were analyzed together as the mean DNAm value. Technical replicates showing $> 5\%$ from the median value were excluded, and the DNAm values from the remaining two replicates were used in the further analyses. Samples with two or three unsuccessful replicates were excluded.

3'mRNA sequencing (mRNA-seq) analysis**Differential expression analysis**

Drop-seq pipeline [41] was used to construct the mRNA-seq count table for available placental (all PAE $n = 64$, early PAE $n = 23$, and control $n = 41$), hESC (H1: alcohol-exposed $n = 7$ and control $n = 6$, Regea08/017: alcohol-exposed and control $n = 6$, respectively), and differentiated male H1 hESC (control/alcohol-exposed endoderm $n = 4/3$, mesoderm $n = 3/3$, and ectoderm $n = 4/4$) RNA samples provided by FuGU. A total of 38,434 transcripts were identified for downstream analysis of placental and 30,081 transcripts of hESC samples. Principal component analysis (PCA) implemented in DESeq2 [42] was used to identify batch effects, and ComBat-seq [43] was used to adjust separate mRNA-seq batches. Differential expression analysis was performed by DESeq2 R package, with model adjusting for smoking and sex for placental samples and with model adjusting cell line for

hESCs. Genes were considered as differentially expressed when FDR-corrected P -value was < 0.05 . Benjamini-Hochberg procedure was used to control for FDR. To validate the hESC differentiation into the germ layer cells, normalized counts of marker genes were used in heatmap visualization (Additional file 2: Fig. S2).

Pathway analyses

enrichgo function in R package clusterProfiler version 4.0 [44] was used to perform gene-set enrichment analysis for significant differentially expressed genes. The GO knowledgebase was used as the source for identifying significantly enriched BP terms (FDR-corrected q -value < 0.05). Benjamini-Hochberg procedure was used to control for FDR.

Correlation analysis

Normalized genome-wide DNAm data was compared to similarly adjusted mRNA-seq data to discover genes, which DNAm changes correlate with mRNA expression in the placenta and hESCs. A total of 53 PAE and 39 control placental samples as well as eight alcohol-exposed and eight control hESC samples (H1 and Regea08/017: $n = 4$ /condition, respectively), of which DNAm and mRNA expression data were available, was used. DNAm and expression data were adjusted to include only the same identified genes between the analyses. For placental data, a total of 126,810 probes were clustered according to 14,635 genes, which were identified from the mRNA-seq data. For hESCs, 106,341 probes were clustered according to 14,051 genes. MethylMix version 2.20.0. R package [45] was used to perform correlation analysis.

Common genes in genome-wide DNAm and mRNA-seq analyses

The gene name annotation information from DNAm (all differentially methylated CpGs with FDR < 0.05) and mRNA-seq (FDR < 0.05) analyses of placenta and hESCs were used to explore the common genes that associate significantly with alcohol exposure. When CpG was annotated to multiple genes, the first UCSC gene name were chosen. If the UCSC gene name was missing, the GENCODE database information was used. GO:BP enrichment analysis of the common genes was performed by R package clusterProfiler version 4.0 (see mRNA-seq pathway analysis).

ChIP-qPCR

ChIP was performed for ~5 million hESCs as described in Schmidt et al. [46] with some modifications using H1 and Regea08/017 cell lines. Two replicates of both cell lines were used, which is four replicates of alcohol-exposed and control ChIP samples in total. Briefly, cells

were cross-linked using 1% formaldehyde and sonicated with Bioruptor[®] Pico sonication device (Diagenode) using optimized parameters 4 cycles of 30s on/90s off to generate DNA fragments of 300–600 bp. For immunoprecipitation, 0.75 mg of Dynabeads[™] Protein G magnetic beads (Invitrogen) were first incubated with 5 μ g of antibodies against H3K4me3, H3K4me2, H3K9ac, and H3 (Additional file 1: Table S6). Subsequently, the shared chromatin was incubated with antibody-bound protein G beads overnight at 4 °C with rotation. The protein-DNA complexes were then washed, eluted, reverse cross-linked, and treated with Proteinase K and RNase A (Thermo Scientific). Finally, the DNA was purified using QIAquick PCR Purification Kit (Qiagen) and used as a template for quantitative PCR (qPCR). The qPCR was performed in triplicates of 10 μ l reactions using SsoAdvanced[™] Universal SYBR[®] Green Supermix (Bio-Rad Laboratories) according to the manufacturer's instructions. The enrichment was normalized against input and further against total histone H3 enrichment. To compare the enrichment between alcohol-exposed and control samples, the data were also normalized against a negative control region designated as "Gene desert." Target sequences were designed to incorporate regions at *DPPA2* and *DPPA4* enriched with histone modifications of interest in the H1 hESC line according to the Encyclopedia of DNA Elements (ENCODE) [47]. Primers for the target sequences were designed using Primer3 [48], and primers for the negative control region were obtained from a previous publication [49]. Primers and location of amplicons in the genome, as well as qPCR protocol, are provided in Additional file 1: Tables S4 and S5.

Statistical analysis

All statistical analyses were conducted in R version 4.2.0 [50], IBM SPSS Statistics for Windows, version 27.0 (IBM Corp.), or GraphPad Prism 9 software (GraphPad Software, Inc.). All data are expressed as the mean with \pm SD for a normal distribution of variables. Statistical analyses were performed as described in the figure legends or in the relevant sections. Pearson correlation coefficient was used for normally distributed DNAm data; otherwise, Spearman's rank correlation coefficient was used.

Results

Characteristics of epiFASD cohort

General characteristics of epiFASD cohort including 80 PAE and 100 control newborns as well as their mothers were compared (Table 1, Additional file 1: Tables S1 and S2). PAE newborns had significantly smaller birth weights (SD), lengths (SD), and HCs (SD) compared to control newborns ($P = 0.030$, Mann-Whitney U, $P = 0.044$ and $P = 0.012$, respectively, Student's t test).

Moreover, to explore more specifically the effects of early PAE on the phenotype as well as placental epigenome and gene expression, we selected 27 newborns whose mothers had consumed alcohol up to GW 7 at maximum to the separate analyses. Notably, also the newborns in this early PAE subgroup had significantly smaller HCs (SD) compared to controls ($P = 0.016$, Student's t test).

When potential correlations between changes in placental weight (g), birth measures (SDs), and maternal alcohol consumption determined by AUDIT scores [18] or ad were calculated between the PAE as well as early PAE newborns and controls, a negative correlations between AUDIT scores and birth length (SD) were found ($r = -0.505$, $P < 0.001$, $n = 44$, $r = -0.576$, $P = 0.012$, $n = 18$, respectively, Spearman's rank correlation). The gestational age was significantly shorter in PAE pregnancies compared to the controls ($P < 0.001$, Mann-Whitney U). Furthermore, the mothers of PAE newborns had significantly higher pre-pregnancy BMI, but gained significantly less weight during pregnancy than the mothers of control newborns ($P = 0.008$, Student's t test and $P = 0.008$, Mann-Whitney U , respectively). However, the weight gain in both groups was within the recommended range [51].

Effects of PAE on genome-wide DNAm in the placenta

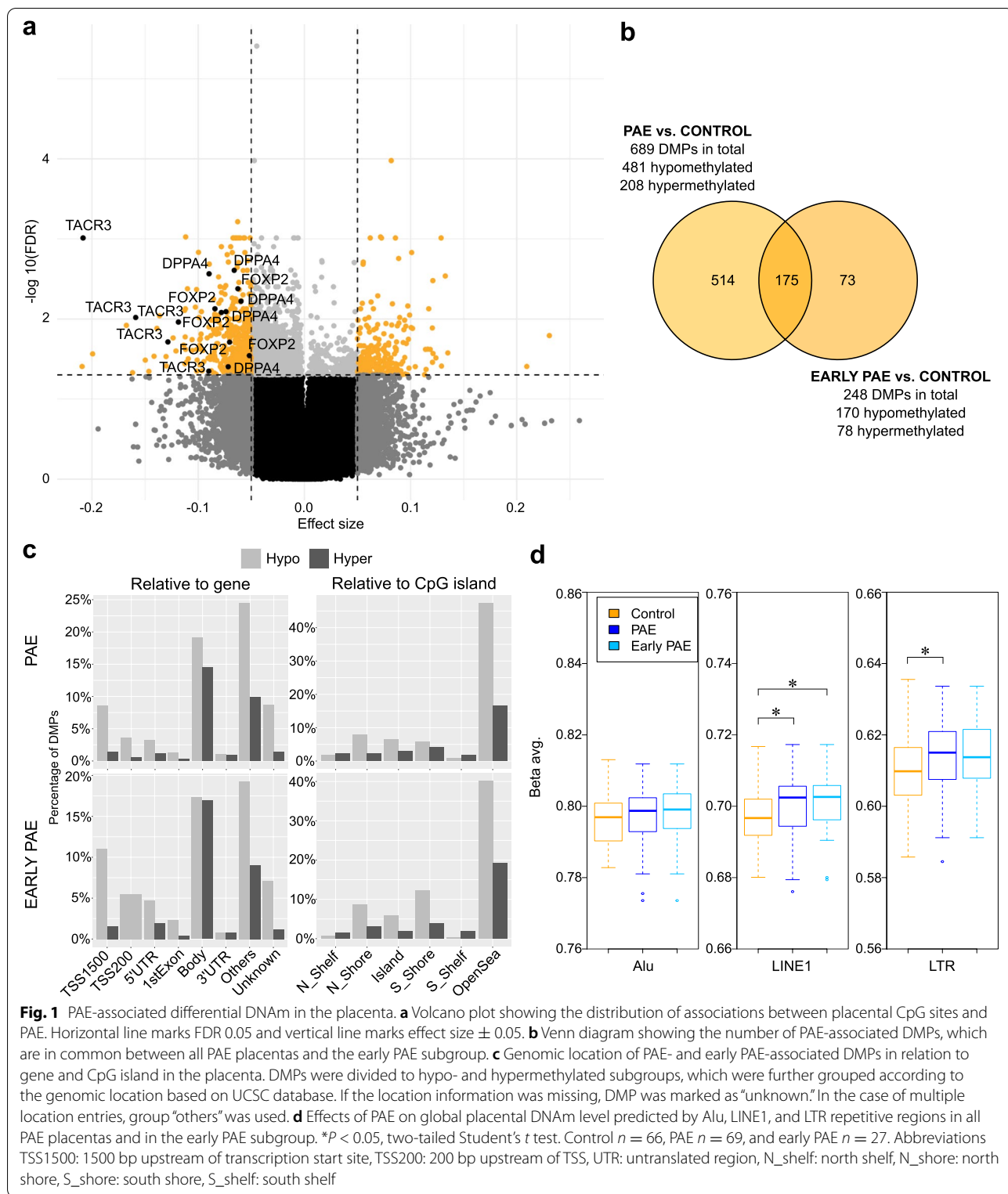
We used Illumina's Infinium MethylationEPIC microarrays to identify PAE-associated genome-wide DNAm alterations in 69 PAE and 66 control full-term placentas (Samples in Additional file 1: Tables S1 and S2, and general characteristics in Additional file 1: Table S3). By adjusting for batch, sex, and smoking covariates, the analysis resulted in 2538 significantly differentially methylated CpG sites (2138 hypomethylated and 400 hypermethylated) with $FDR < 0.05$ (Fig. 1a,b and Additional file 1: Table S7). To separate the most prominent changes and to minimize false positive hits ($\lambda = 1.69$, Additional file 2: Fig. S3a), we focused on the CpG sites with DNAm difference of $\geq 5\%$ between PAE and control placentas, which are termed as differentially methylated positions (DMPs). There were 689 DMPs associated with PAE ($FDR < 0.05$, $\Delta\beta \leq -0.05$ and $\Delta\beta \geq 0.05$), of which 481 were hypomethylated and 208 hypermethylated. The PCA performed for DMPs indicated that although observed alterations associate with PAE, smoking appeared to be a strong confounding factor (Additional file 2: Fig. S5).

The analysis revealed five hypomethylated DMPs in *DPPA4*. Furthermore, *transcription factor forkhead box P2* (*FOXP2*), which is needed for the development of speech regions in the brain during embryogenesis [52, 53], had six hypomethylated DMPs, and *Tachykinin Receptor 3* (*TACR3* or *neurokinin 3 receptor*, *NK3R*) expressed in the central nervous system had

five hypomethylated DMPs. Interestingly, genetic polymorphisms in *TACR3* have been previously associated with alcohol and cocaine addiction [54], and hypomethylation of the promoter region in blood is linked to repeated cocaine administration in marmoset monkeys [55]. The observed DMPs were mainly located in regulatory regions and in the first exons (Additional file 1: Table S7). Furthermore, all three candidate genes were associated with PAE in sensitivity analyses, in which known potential confounding factors were excluded (Additional file 1: Tables S8 and S9), and their effect sizes were consistently altered in all performed analyses (Additional file 2: Fig. S6).

In addition to testing for associations for each CpG separately, we tested for differentially methylated regions (DMRs) defined as a region with maximal allowed genomic distance of 1000 bp containing three or more CpGs of which at least one CpG with a $\Delta\beta \leq -0.05$ or $\Delta\beta \geq 0.05$. A total of 112 DMRs were observed, including highly significantly hypomethylated DMRs in *DPPA4* (6 CpGs), *FOXP2* (7 CpGs), and *TACR3* (10 CpGs) (Additional file 1: Table S10). Previously, *FOXP2* and *TACR3* have been linked to PAE-associated hypomethylated DMRs in mouse hippocampus [56] and rat prefrontal cortex [57], respectively. Furthermore, the DMP and DMR analyses brought forth several interesting genes such as *ANK3*, *CCDC3*, *WNT3*, *PALMD*, and *SEMA3B*, of which *PALMD* associated with PAE also in sensitivity analysis for DMPs (Additional file 1: Table S8). Regarding the retarded growth associated with FASD, previous associations between PAE and *IGF2/H19* locus [16, 58–60], and our earlier finding on the genotype-specific effects of PAE on DNAm of imprinting control region in *IGF2/H19* locus in the placenta [61], also DMR in *IGF2/IGF2AS* (21 CpGs) observed in the current genome-wide study with a larger sample size is highly interesting. This hypomethylated DMR spans 1756 bp and locates in the first exon of *IGF2* (Additional file 2: Fig. S7).

We also performed genome-wide DNAm analyses of placentas in the early PAE subgroup ($n = 27$). The analysis revealed 248 PAE-associated DMPs (170 hypomethylated and 78 hypermethylated, $FDR < 0.05$, $\Delta\beta \leq -0.05$ and $\Delta\beta \geq 0.05$) (Fig. 1b and Additional file 1: Table S11 as well as Tables S12 and S13 for sensitivity analyses), including hypomethylated DMPs in *DPPA4* and *TACR3* (two and six DMPs, respectively). Interestingly, two genes, *A2BPI* (also known as *RBFOX1*) and *DIP2C*, of which DMPs were observed in the early PAE placentas, have also been associated with altered DNAm in WBCs of early PAE newborns in previous meta-analysis of six population-based birth cohorts (P -values were not significant after multiple testing correction in this study) [62]. In both placenta and WBCs, there were hypermethylated



DMP/CpG in the regulatory region of *A2BP1*, and hypo-methylated DMP/CpG at the gene body of *DIP2C*—although not the same probes. Both genes have been

associated previously with neuronal development and autism spectrum disorders (ASD) [63, 64]. DMR analysis for the early PAE subgroup revealed 29 DMRs, including

DPPA4 (4 CpGs) and *TACR3* (10 CpGs) (Additional file 1: Table S14).

Previously, PAE has been associated with altered cellular composition in human term placenta [65]. Therefore, although we study developmentally early alterations, which are expected to be present in subsequent cell lines derived from early developmental cell types exposed to PAE and consequently could be used as biomarkers, we excluded a potential bias in the results caused by cellular composition by cell-type-specific adjustment. Significantly increased proportions of trophoblast cells observed in all PAE placentas as well as in the early PAE subgroup compared to controls ($P = 0.006$, $P = 0.038$, respectively, Wilcoxon test) (Additional file 2: Fig. S8) are consistent with the PAE-associated increased number of villous cytotrophoblastic cells observed in the previous study [65]. Furthermore, the number of stromal cells was significantly lower in both groups of PAE placentas ($P < 0.001$, $P < 0.001$, respectively, Student's t test) (Additional file 2: Fig. S8). However, the results of cell-type-specific DNAm analyses were consistent with the bulk results and confirmed the significance of the candidate genes *DPPA4*, *FOXP2*, and *TACR3* (Additional file 1: Tables S15–18).

Prominent PAE-associated hypomethylation of DMPs was observed in the majority of genomic locations relative to gene and CpG island in all PAE placentas—especially in the regulatory regions of placentas in the early PAE subgroup (Fig. 1c). In all PAE placentas, in relation to gene or CpG island, DMPs were enriched at the open sea (64.0% of the DMPs vs 56.7% in the EPIC array) and under-represented in the CpG island (9.3% vs 17.5%). In the subgroup of early PAE placentas, DMPs were enriched at the first exon (2.8% vs 1.0%) and south shore (16.1% vs 8.7%), and under-represented in CpG island (8.1% vs 17.5%) ($P < 0.0001$, $P < 0.0001$, $P = 0.015$, $P = 0.0002$, $P < 0.0001$, respectively, Fisher's exact test followed by pairwise comparisons). The effect of PAE on genome-wide placental DNAm level was calculated by using 588,781 probes in the array, and significantly lower overall GWAM was observed in all PAE placentas compared to controls ($P = 0.012$, Student's t test). This hypomethylation was seen in all genomic locations in both all placentas and the early PAE subgroup (Additional file 2: Fig. S9). The global placental DNAm level was also predicted by comparing the mean DNAm level of CpGs in Alu, LINE1, and LTR repetitive element regions, which comprise 36% of human genome in total [38, 66]. On the contrary to the hypomethylation observed when using DMPs or GWAM, significant hypermethylation was observed at LINE1 and LTR regions in all PAE placentas ($P = 0.019$ and $P = 0.02$, respectively, Student's t test) and in LINE1s in the early PAE subgroup ($P = 0.029$, Student's t test) compared with controls (Fig. 1d).

Pathway analyses were performed to get a comprehensive picture on the biological processes in which PAE-associated DMPs cluster. GO enrichment analysis of PAE-associated DMPs revealed interesting BPs involved in the function of heart and nervous system as well as adult behavior ($P < 0.05$) (Fig. 2a and Additional file 1: Table S19). DMRs cluster to various BPs, such as the regulation of chemotaxis, embryonic placenta morphogenesis, Wnt signaling in stem cell proliferation, and putamen and caudate nucleus development ($P < 0.05$) (Fig. 2b and Additional file 1: Table S20). Both DMPs and DMRs cluster to the GO terms involved in vocalization behavior and genomic imprinting.

Potential biomarkers for PAE

To validate the results of genome-wide DNAm microarray analysis and to determine potential biomarkers for PAE, we examined DNAm profiles of *DPPA4*, *FOXP2*, and *TACR3* in placenta, WBCs, and BECs from each newborn by targeted DNAm analysis using EpiTYPER (Agena Bioscience, Inc.). Targets for the EpiTYPER analysis were selected based on the microarrays and the significance of the identified DMPs when all PAE placentas were compared to controls. Noteworthy, the normalized (not adjusted for smoking and sex) sample-specific DNAm levels were used in this analysis. There was a significant difference in the DNAm levels of *DPPA4* between control and all PAE placentas (cg13358761: $P = 0.009$, cg14836960: $P = 0.002$, and cg07253829: $P = 0.003$, cg08881331: $P = 0.042$, Student's t test) (Fig. 3a). Interestingly, the difference was even more significant in the early PAE subgroup, which suggests early origin of these changes (cg13358761: $P < 0.001$, cg14836960: $P = 0.001$, and cg07253829: $P < 0.0001$, cg08881331: $P = 0.015$, Student's t test). Although some significant differences in the normalized DNAm levels of *FOXP2* or *TACR3* were detected (cg18871253 (all PAE placentas): $P = 0.047$, and cg16461251 (early PAE subgroup): $P = 0.047$, respectively) the differences were smaller than expected. Considering the significance of these genes in the sensitivity analyses without smoking-exposed samples (adjusted only for sex), we tested the effect of sex on the DNAm levels of the DMPs with the largest effect size (Fig. 3b). Interestingly, when we compared DNAm levels between males and females, we observed significant sex-specific effects in *FOXP2* in both all PAE placentas and in the early PAE subgroup ($P = 0.01$, $P = 0.023$, respectively, Student's t test).

The placental samples with the largest DNAm difference between PAE and control groups were chosen for the further analysis (*DPPA4* (cg14836960) and *TACR3* (cg16461251) $P < 0.001$, *FOXP2* (with two DMPs in the same unit: cg18871253 and cg24786986) $P = 0.002$,

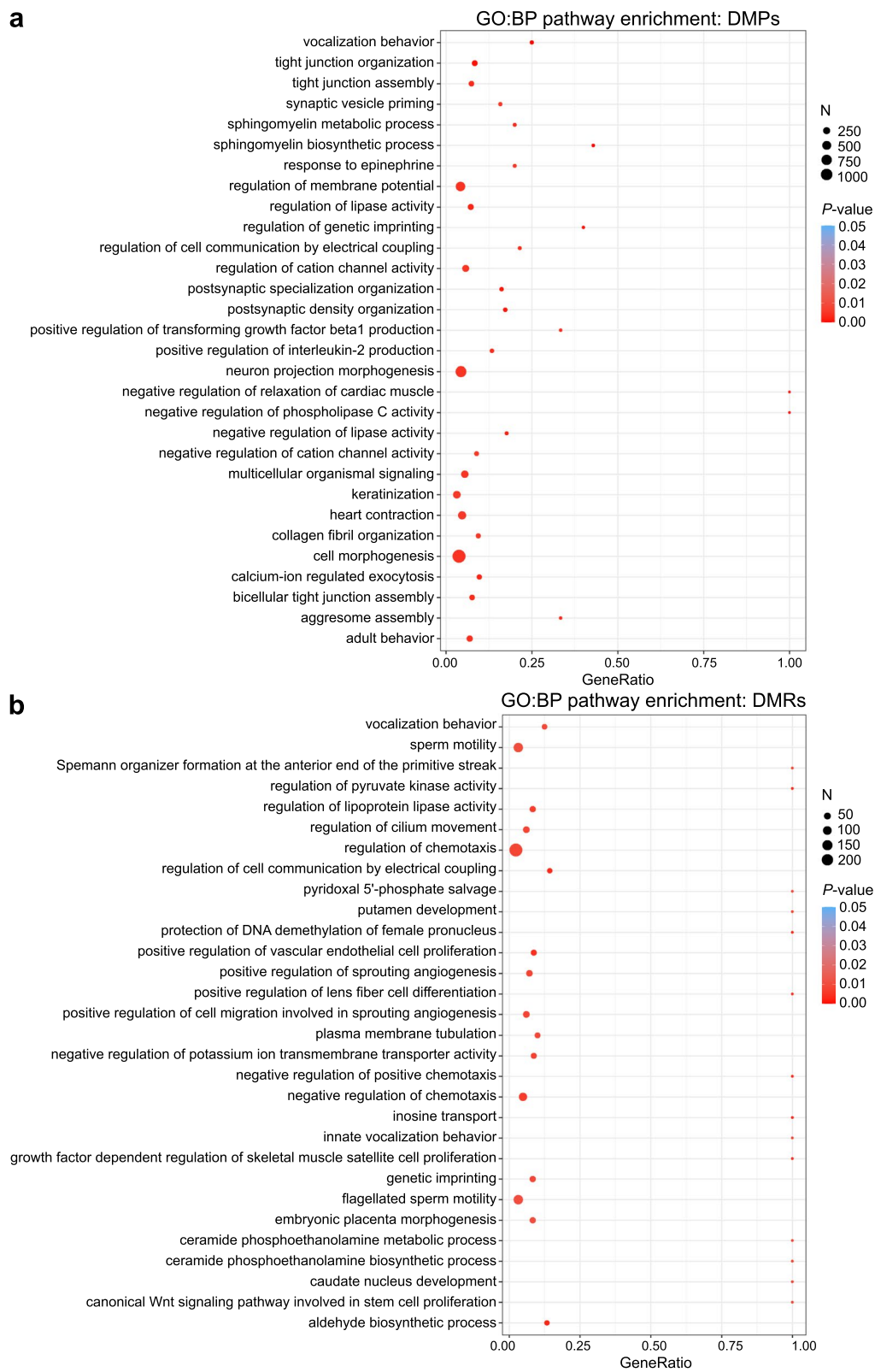


Fig. 2 Pathway analyses of placental DMPs and DMRs. Enriched terms identified in GO:BP enrichment analysis of PAE-associated **a** DMPs and **b** DMRs in placenta ($P < 0.05$). In both figures the 30 most significant pathways are shown

Mann-Whitney *U*, Additional file 1: Table S21, selected samples in the Additional file 1: Tables S1 and S2). The DNAm levels of selected DMPs in placenta measured by the microarrays and EpiTYPER correlated significantly, and thus validated the DNAm results as well as the feasibility of the selected EpiTYPER primers (*DPPA4*: $r = 0.856$, $P = 3.29 \times 10^{-9}$, $n = 29$; *FOXP2*: $r = 0.962$, $P = 4.72 \times 10^{-11}$, $n = 19$; and *TACR3*: $r = 0.903$, $P = 4.06 \times 10^{-6}$, $n = 15$, respectively, Spearman's rank correlation).

We next examined the applicability of observed PAE-associated placental DNAm differences for potential PAE biomarkers in blood or BECs, which are more easily accessible biological samples than placenta. The stability of DNAm levels across placenta, WBCs, and BECs from each of the selected newborns was tested, but significant correlations between tissues or cell types were not observed. However, when only the PAE newborns with the lowest placental DNAm level of *DPPA4* DMP (cg14836960) were scrutinized, a trend of low DNAm level was detected also in BECs of the same newborns (Fig. 3c). Furthermore, a trend of PAE-associated hypomethylation of DMP in the first exon of *TACR3* (cg16461251) was observed also in WBCs and BECs (Fig. 3c). Notably, the DNAm difference in this specific DMP between selected control and PAE placentas was also significant in BECs analyzed by EpiTYPER ($P = 0.009$, Mann-Whitney *U*).

Effects of PAE on placental mRNA expression

To study genome-wide PAE-associated alterations in gene expression, we performed mRNA-seq for 64 PAE and 41 control placentas (Samples in Additional file 1: Tables S1 and S2, and general characteristics in Additional file 1: Table S3). When the mRNA-seq model was adjusted by smoking and sex, we observed 114 significantly differentially expressed genes (FDR < 0.05) of which 41 were downregulated and 73 upregulated (Fig. 4a,b and Additional file 1: Table S22). According to the GO:BP enrichment analysis, PAE-associated gene expression is linked predominantly to cellular respiration in mitochondria (FDR-corrected q -value < 0.05) (Fig. 4c and Additional file 1: Table S23). Indeed, the majority of the most

significantly differentially expressed genes (FDR < 0.01) have roles in mitochondrial function and cellular respiration (*MICOS13*, *MT-TV*, *COX5B*, *SERP1*, *MRPL54*, *MRPL27*, *NDUFB7*, *GSTP1*, and *NDUFS8*), in increasing the level of reactive oxygen species (ROS) (*ROMO1*) [67] as well as in cellular response to oxidative stress (*PAG1*) [68] and hypoxia (*HIF3A*) [69]. This is consistent with previous studies, since alcohol exposure has been associated with increased oxidative stress and mitochondrial dysfunction in several tissues [70, 71], including rat placenta [72]. Increased oxidative stress is characteristic for several gestational disorders such as intrauterine growth restriction and preterm birth [73, 74], which are also known characteristics of PAE. According to our analysis, *DPPA2*, *DPPA4*, *FOXP2*, or *TACR3* are expressed below the detectable level in the term placenta.

Three genes, *DKK1*, *RBP4*, and *UCHL1*, were significantly upregulated in the placentas of the early PAE subgroup ($n = 23$, FDR < 0.05) (Additional file 1: Table S24). *Dickkopf1* (*DKK1*), which was significantly upregulated also in all PAE placentas (Fig. 4a,b), is crucial for head, limb, and heart development [75, 76]. It is an inhibitor of the Wnt/ β -catenin signaling pathway [77], which among various developmental processes has an essential role in the development of early trophoblasts [78]. Interestingly, increased expression of *DKK1* has been associated previously with pre-eclampsia [79, 80] and unexplained recurrent spontaneous miscarriage [81].

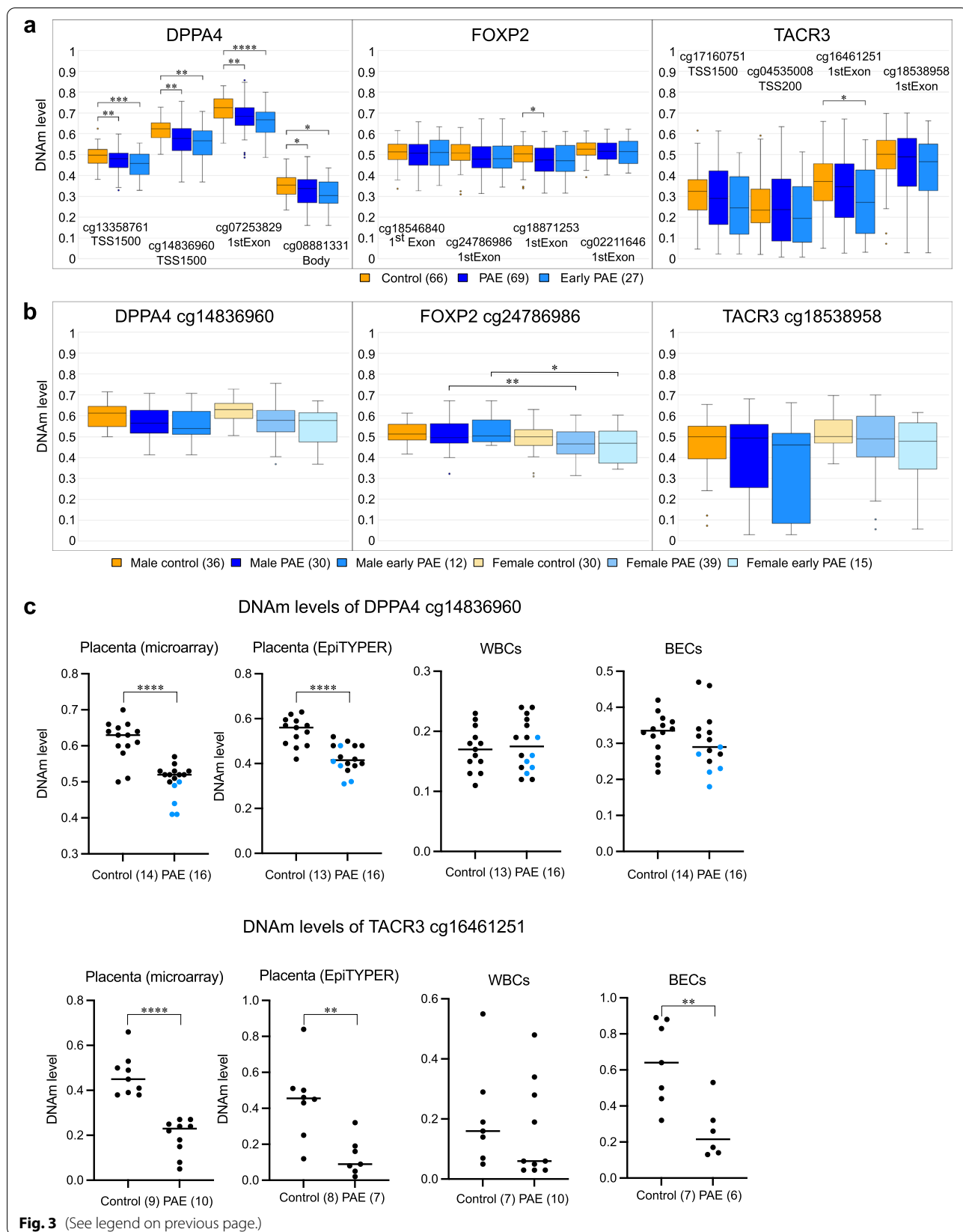
To characterize the potential effect of PAE-associated DNAm on gene expression levels in the same samples, we performed correlation analysis. The analysis revealed nine genes, which had significant PAE-associated correlation between decreased DNAm and increased mRNA expression in the placenta: *B3GNT3*, *CBR1*, *CNDP2*, *HEATR5A*, *PRKAG2*, *S100A14*, *SAR1B*, *STEAP3*, and *TUSC3* ($P < 0.01$) (Additional file 1: Table S25). All the genes, except *B3GNT3* and *PRKAG2*, have correlative probes in the regulatory regions.

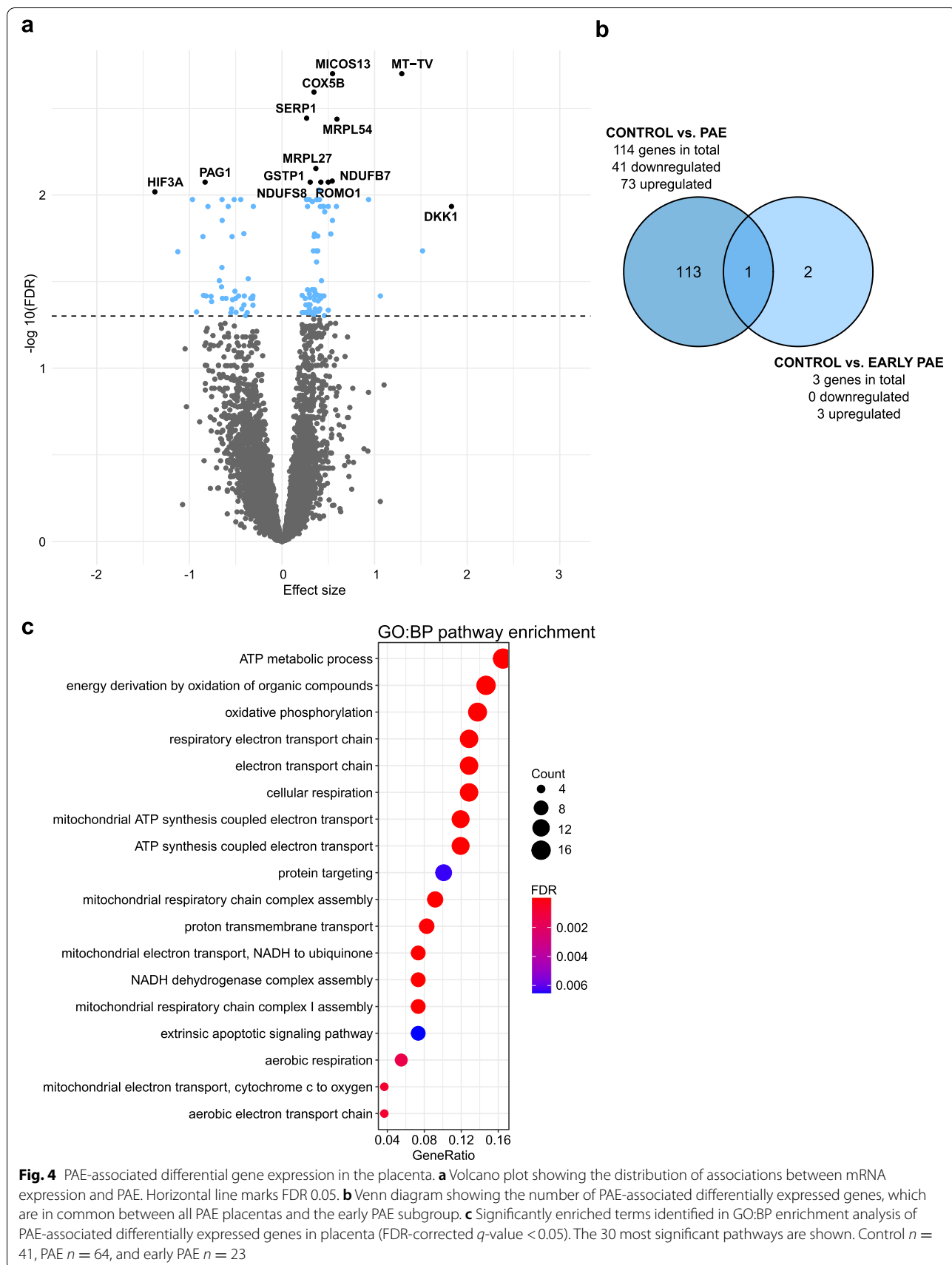
Effects of in vitro alcohol exposure on hESCs

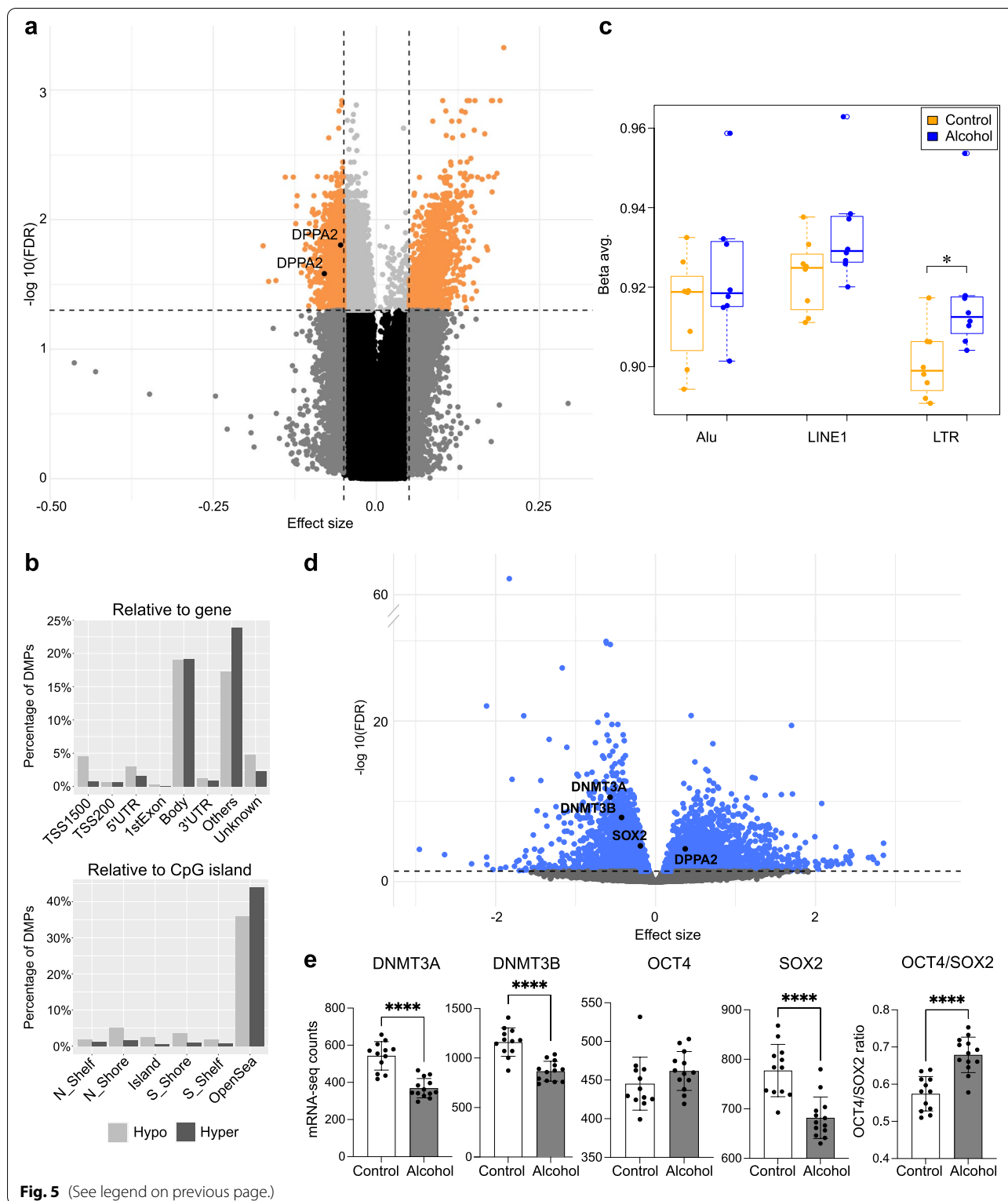
To explore the effects of early alcohol exposure on hESCs without potential confounding factors associated with human studies in vivo, we exposed two cell lines (H1 and

(See figure on next page.)

Fig. 3 DNAm levels of potential PAE biomarkers *DPPA4*, *FOXP2*, and *TACR3*. **a** Box plots showing the normalized DNAm levels of DMPs and their locations in relation to gene in *DPPA4*, *FOXP2*, and *TACR3* in control, PAE, and early PAE placentas. Four DMPs with the largest effect sizes (mean $\Delta\beta$) based on linear model of each candidate gene are presented. * $P < 0.05$, ** $P < 0.01$, *** $P < 0.001$, **** $P < 0.0001$, two-tailed Student's *t* test. **b** Box plots showing sex-specific normalized DNAm levels of DMPs with the largest effect sizes. * $P < 0.05$, ** $P < 0.01$, two-tailed Student's *t* test. **c** DNAm levels of *DPPA4* DMP (cg14836960) and *TACR3* DMP (cg16461251) in selected placental samples analyzed by microarrays and EpiTYPER as well as the same CpGs in WBCs and in BECs analyzed by EpiTYPER. Blue dots in *DPPA4* indicate DMP of each PAE placenta, which have the lowest DNAm levels in microarrays. ** $P < 0.01$, **** $P < 0.0001$, Mann-Whitney *U*







unmethylated in both alcohol-exposed and control hESCs (Fig. 5a and b, Fig. 6b) (confirmed by EpiTYPER analysis, Additional file 1: Table S33). Furthermore, we studied

potential alcohol-induced alterations in histone modifications H3K4me2, H3K4me3, and H3K9ac by ChIP-qPCR. The trends of the observed changes were consistent with the

alcohol-induced alterations in DNAm and gene expression, but they were not statistically significant. Although the level of histone modifications in the regulatory region of *DPPA2* was very low compared to *DPPA4*, we observed increased amount of active chromatin mark H3K4me2 in the regulatory regions of both *DPPA2* and *DPPA4* as well as increased amount of H3K4me3 in *DPPA4* in alcohol-exposed hESCs (Fig. 6c).

To see the potential effects of alcohol exposure on DNAm profiles of *DPPA2* and *DPPA4* regulatory regions in differentiating cells, we differentiated hESCs (H1) into the endodermal, mesodermal, and ectodermal cells in vitro. The cells were exposed to 70 mM alcohol during the culturing and the DNAm profiles of *DPPA2* and *DPPA4* loci were analyzed from normalized Illumina's EPIC microarray data (four alcohol-exposed and four control samples/germ layer). The DNAm profile of endodermal cells was similar to hESCs with significant locus-specific decreased DNAm in *DPPA2* regulatory region in alcohol-exposed cells and unmethylated *DPPA4* regulatory region in both alcohol-exposed and control cells (Fig. 6d). On the contrary to the hESCs, increased DNAm level in the *DPPA4* regulatory region was observed in mesodermal and ectodermal cells. Notably, consistent with the PAE placentas, both mesodermal and ectodermal cells had significant locus-specific alcohol-induced decreased DNAm in the regulatory region of *DPPA4* (Fig. 6d,e).

Genome-wide effects of in vivo and in vitro alcohol exposure

Finally, to see the early effects of alcohol exposure on genes in both in vivo exposed extraembryonic placenta and in vitro exposed hESCs, we compared the results of genome-wide DNAm and mRNA-seq analyses (Fig. 7a and Additional file 1: Table S34). The comparisons were performed by using all significant CpGs (FDR < 0.05) and significantly differentially expressed genes (FDR < 0.05). Only one common gene, *TBC1 domain family member 5* (*TBC1D5*), associated with alcohol exposure in all genome-wide analyses of placenta and hESCs. *TBC1D5* encodes a GTPase-activating protein involved in hepatic lipophagy [83], which protects the liver from alcohol-induced fatty liver disease [84]. It has been shown to be downregulated by chronic alcohol administration in mouse liver and ethanol-treated HepG2 cells [85]. In the current study, *TBC1D5*

was downregulated in PAE placentas (one hypomethylated CpG in 5'UTR) but upregulated in alcohol-exposed hESCs (two hypomethylated CpGs in the gene body).

A total of 494 common genes associated significantly with alcohol exposure in DNAm analyses of placenta and hESCs. Notably, according to the GO:BP enrichment analysis, these common genes are linked exclusively to neurodevelopmental GO terms including axon development and synapse organization (FDR-corrected q -value < 0.05) (Fig. 7b and Additional file 1: Table S35). Importantly, several of these common genes have been previously associated with PAE or FASD in BECs or/and peripheral WBCs in children (Additional file 1: Table S36). *PTPRN2* [86], *MAD1L1* [87], and *AGAP1* [88] are all linked to neurodevelopmental disorders and associate significantly with PAE or FASD in two or more previous genome-wide DNAm studies [16, 17, 62, 89]. Furthermore, *FOXP1*, a family member of *FOXP2*, and *GLI2* have been found to associate with FASD diagnosis in BECs [89] or WBCs [15] in childhood, respectively. Interestingly, transcription factor *GLI2* is a mediator of Sonic hedgehog signaling, and it has been earlier associated with facial dysmorphism and brain deficiency in alcohol-exposed mouse fetuses [90].

Associations between candidate genes, alcohol consumption, and newborns' phenotypes

Potential correlations between placental DNAm and gene expression of the candidate genes and maternal alcohol consumption were calculated. DMPs with the largest effect sizes were examined. A moderate negative correlation between *TACR3* DNAm and ad was observed in the all PAE group (cg16461251: $r = -0.403$, $P = 0.041$ and cg18538958: $r = -0.395$, $P = 0.046$, $n = 26$, Spearman's rank correlation) and a strong negative correlation in the early PAE subgroup (cg18538958: $r = -0.762$, $P = 0.028$, $n = 8$, Spearman's rank correlation). When the correlations between placental DNAm and newborns' birth measures (SDs) and placental weight (g) were examined, no correlations in the all PAE group were detected. However, in the early PAE subgroup, *DPPA4* and *FOXP2* DNAm correlated moderately and negatively with the birth weight (cg14836960: $r = -0.431$, $P = 0.025$, cg18546840: $r = -0.415$, $P = 0.032$, respectively, $n = 27$, Pearson correlation). Also, *FOXP2* DNAm correlated moderately and negatively with the birth length ($r = -0.466$, $P = 0.014$, Pearson correlation). Interestingly, the *DPPA4* DMP (cg14836960) correlated significantly with

(See figure on next page.)

Fig. 6 Effects of alcohol exposure on *DPPA2* and *DPPA4* in hESCs and differentiating cells. **a** *DPPA2* and *DPPA4* gene expressions in control ($n = 12$) and alcohol-exposed ($n = 13$) hESCs. **b** *DPPA2* and *DPPA4* DNAm profiles in control and alcohol-exposed hESCs ($n = 8$ /condition). **c** *DPPA2* and *DPPA4* histone modifications in control and alcohol-exposed hESCs ($n = 4$ /condition). Histone modification enrichments were normalized to the total histone H3. **d** *DPPA2* and *DPPA4* DNAm profiles in control and alcohol-exposed differentiated endo-, meso-, and ectodermal cells ($n = 4$ /condition, respectively). **e** *DPPA2* and *DPPA4* DNAm profiles in control ($n = 66$) and PAE ($n = 69$) placentas. Data presented as mean \pm SD. * $P < 0.05$, Mann-Whitney U and **** $P < 0.0001$, FDR-corrected P -value

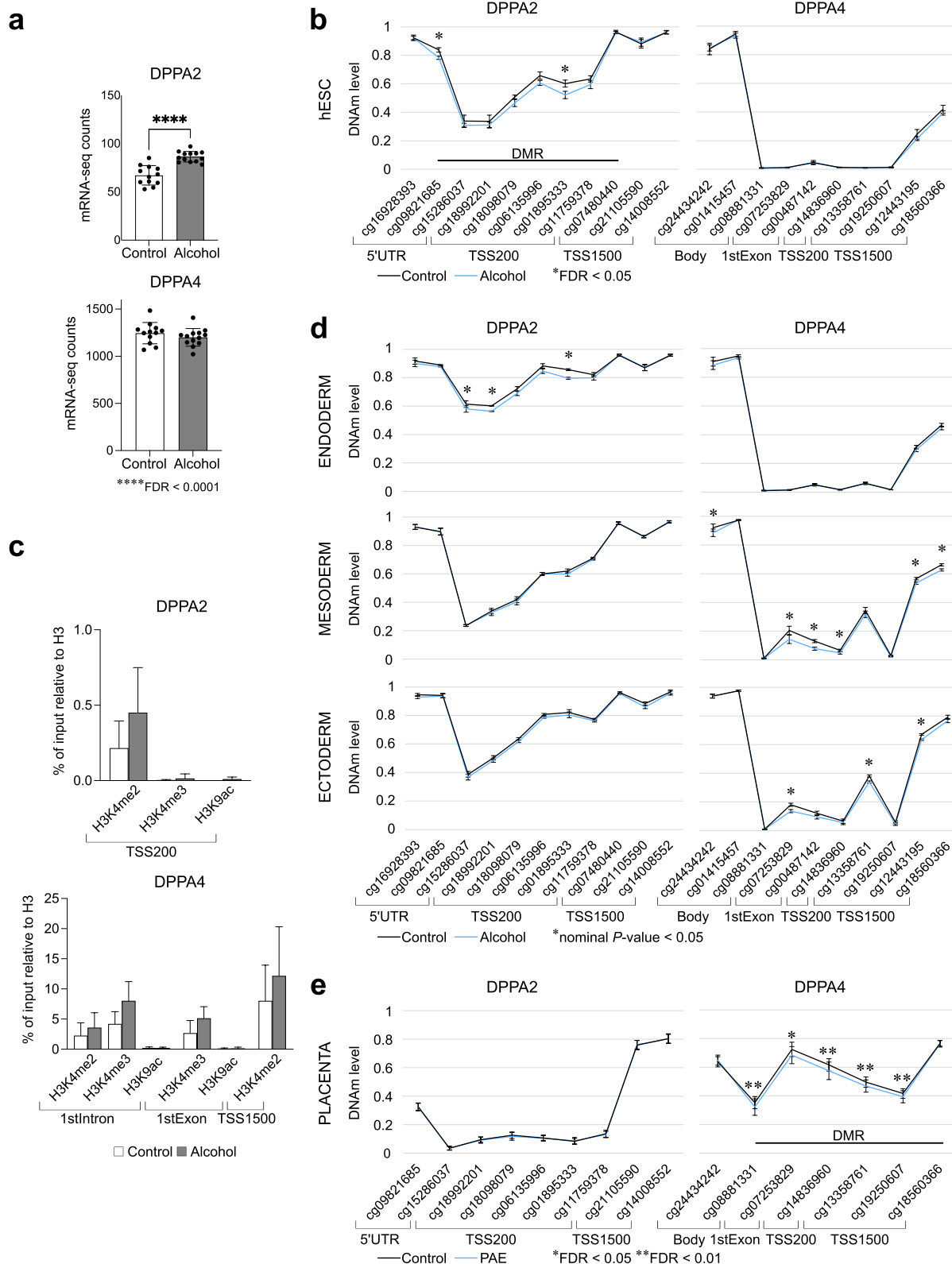
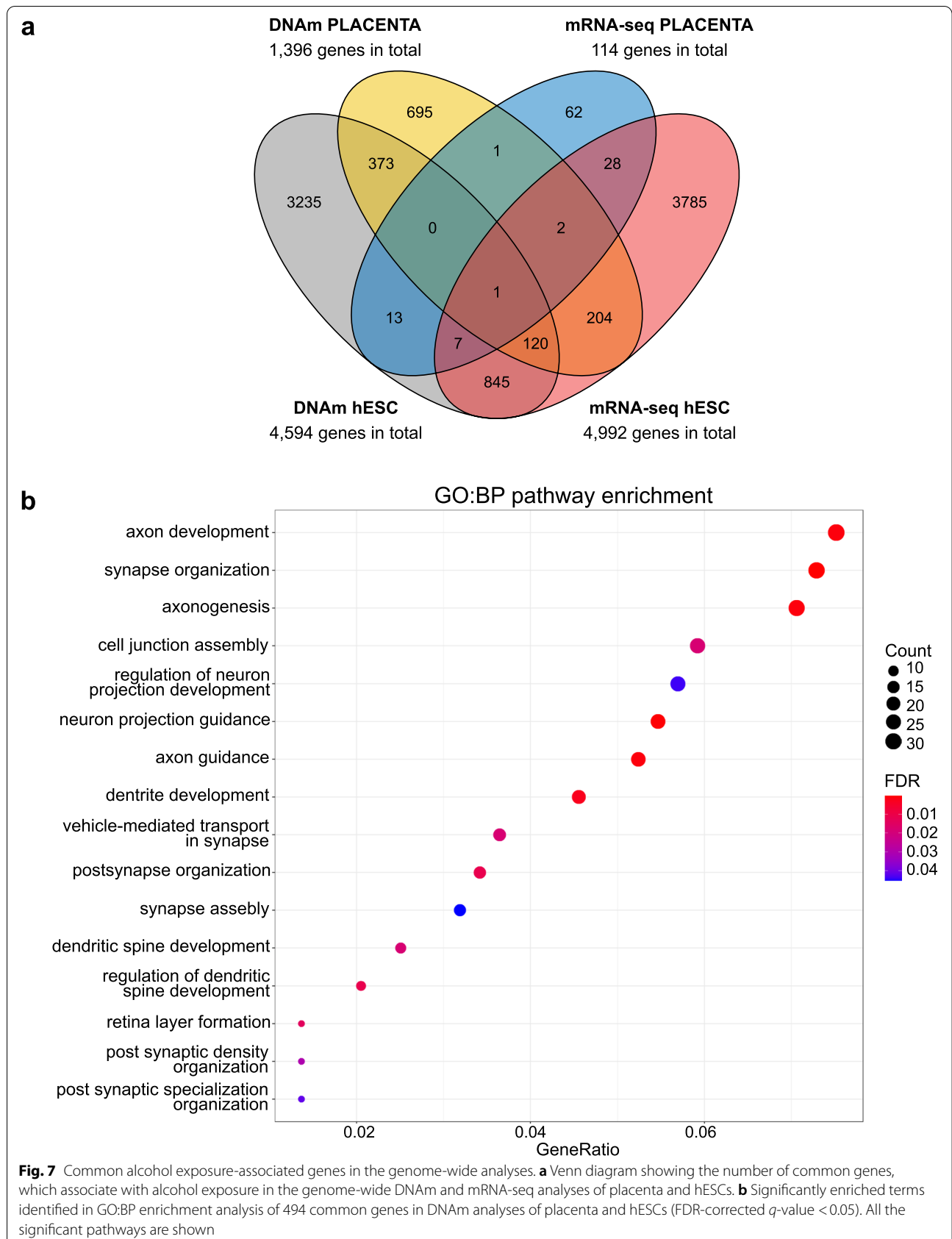


Fig. 6 (See legend on previous page.)



FOXP2 (cg18546840: $r = 0.491$, $P = 0.009$, cg24786986: $r = 0.466$, $P = 0.0014$, respectively, $n = 27$, Pearson correlation) and *TACR3* (cg16461251: $r = 0.415$, $P = 0.031$, $n = 27$, Pearson correlation) DMPs in the early PAE subgroup, but no correlations were observed in the all PAE placentas group. Also, the potential effect of alcohol consumption on genome-wide DNAm was calculated, but no correlation between GWAM and AUDIT scores or ad were found.

Discussion

Our study, which is the first genome-wide DNAm analysis of severely alcohol-exposed placentas as far as we are aware, strengthens the value of placental tissue in studying the effects of prenatal environment on human development. This can be seen in similar locus-specific DNAm alterations in *DPPA4* and *TACR3* in alcohol-exposed extraembryonic and embryonic cells as well as in similar global DNAm changes in both in vivo and in vitro exposed cell types. Also, the common genes with alcohol-associated DNAm changes in placenta and hESCs were linked to the neurodevelopmental pathways. Alterations in genes involved in axon development or synapse organization may not be essential for placental cells, but DNAm changes can reveal the effects of early environment on epigenome in general, without cell or tissue specificity.

The role of *DPPA2* and *DPPA4* as chromatin modifiers and epigenetic priming factors in early development makes them plausible candidate genes for developmental disorders. Alcohol-induced alteration in the regulation of *DPPA2* in hESCs as well as decreased DNAm in *DPPA4* regulatory region in PAE placentas and alcohol-exposed mesodermal and ectodermal cells indicates that alcohol is able to affect their regulation in the early development. Delayed down-regulation of epigenetic priming factors during a critical period of development can result in subtle but widespread alterations in the timing and efficiency of developmental programming. Indeed, increased levels of both *DPPA2* and *DPPA4* have enhanced reprogramming to pluripotency in mouse and human cells [11] and expression of *DPPA4* has been associated with inhibition of ESC differentiation into a primitive ectoderm lineage in mouse [91]. Furthermore, our study shows that alcohol exposure alters the balance of *OCT4* and *SOX2* expression in hESCs, which is in line with a previous mouse study [8]. Owing to the effects of these two lineage specifier proteins on the differentiation into mesoendoderm or neuronal ectoderm [82, 92, 93], our results are consistent with the idea that alcohol can affect the cell fate decision and consequently reduce the number of ectodermal cells [8]. Observed changes in *DPPA4*, *OCT4*, and *SOX2* could explain the specific vulnerability of the developing nervous system to the effects of alcohol.

Another candidate gene for alcohol-induced developmental disorders identified in the current study is

the transcription factor *FOXP2*, which represses genes involved in maintaining a non-neuronal state and activates genes that promote neuronal maturation by affecting chromatin structure [94]. Neuronal phenotypes associated with *FOXP2* mutations include expressive and receptive language impairment, orofacial dyspraxia, abnormalities in cortex, and basal ganglia [53, 95, 96] as well as attention deficit hyperactivity disorder (ADHD) [97]. Since receptive and expressive language disorders as well as ADHD have been considered common comorbidities of FASD [98, 99], *FOXP2* is a plausible candidate gene for developmental disorders induced by PAE. Interestingly, both *FOXP1* and *FOXP2* as well as their targets have been associated with ASD [100–102], which could explain the partial overlapping phenotypes between FASD, ASD, and ADHD observed in previous studies [98, 103].

The observed difference in *DPPA4* DNAm between PAE and control placentas is a potential biomarker for early alcohol exposure or even FASD, but the use of placental tissue in diagnostics has limitations. The PAE-associated trend of decreased DNAm in *TACR3* in both newborns' placenta and BECs however suggests that alterations are detectable in different tissue types with variable cell-type compositions, which makes buccal swabs a promising tool for diagnostics. Due to the ectodermal origin of BECs, buccal samples could be particularly useful for the diagnostics of neurodevelopmental disorders. However, when placental DMPs were compared to all four previous genome-wide DNAm studies of BECs [16, 17, 89, 104], no common PAE- or FASD-associated probes or genes were found (Additional file 1: Table S37). Although a total of 43 genes in the current study associated with PAE or FASD in some of the previous studies, our three candidate genes, *DPPA4*, *FOXP2*, or *TACR3*, have not been detected earlier. The inconsistency could be explained by the cellular heterogeneity, different age of the affected children, or differences in genetic background. Owing to *TACR3*'s role in growth, reproduction, and several processes in the nervous system [105, 106] as well as the moderate correlation between placental *TACR3* hypomethylation and alcohol units consumed per week, it is also an interesting candidate gene for alcohol-induced developmental disorders. Since genetic variation in *TACR3* has been associated with alcohol dependence [54], potential genotypic effects on observed PAE-associated hypomethylation should be studied in the future. Furthermore, it has been shown previously [107, 108] as well as in this study that PAE has sex-specific effects. Although it was not in the focus of the current study, it requires further investigation.

The majority of the alcohol-associated DMPs in the regulatory regions in both placenta and hESCs were hypomethylated, and also significant alcohol-associated

genome-wide hypomethylation in all genomic locations based on GWAM was observed. On the contrary, by using repetitive elements, we predicted increased global alcohol-associated DNAm in both placenta and hESCs. This is consistent with the previous study, in which PAE throughout the pregnancy has been associated with higher placental global DNAm examined by using Alu repeats of male newborns [109]. Also, the increased DNAm at the LTR promoter of intracisternal A particle in the *agouti* locus was observed in our previous study, in which we showed for the first time that PAE can affect adult phenotype by altering the epigenotype of early mouse embryo [5]. The mechanisms by which alcohol alters the DNAm are still mainly unknown. Enzymatic malfunction of DNMTs caused by oxidative stress or effects of alcohol on cells' methionine cycle and consequently on DNAm level have been suggested in previous studies [110]. Also, according to previous studies, the timing of exposure is fundamental—the effects differ between undifferentiated, differentiating, and differentiated cells [7, 111].

We explored more specifically the effects of early PAE by selecting 27 newborns whose mothers had consumed alcohol up to GW 7 at maximum to the separate analyses. Observed similar trends of PAE-associated DNAm alterations in all PAE placentas as well as in the early PAE subgroup suggest that there are changes that have occurred already in the early pregnancy. Also, the significant correlation of *DPPA4* DNAm with *FOXP2* and *TACR3* only in the early PAE subgroup suggests a parallel effect of early exposure on these three candidate genes in each placenta, which may be confounded during prolonged exposure. Although the birth weight (SD) or length (SD) of the newborns in this subgroup did not differ from controls, their significantly smaller HC (SD) suggests adverse effects of early PAE on brain development. Due to the increasing alcohol consumption among women in child-bearing age [112] and a large proportion (44–65%) of unplanned pregnancies [113], there is a considerable risk of PAE and consequently neurodevelopmental disorders prior to pregnancy recognition. This developmentally critical period, the first weeks of pregnancy from fertilization to gastrulation and to the beginning of organogenesis, should be in the focus of future studies. Especially the role of Wnt signaling in the etiology of FASD should be explored, since this developmentally crucial pathway brought forth in several of our analyses.

We are aware of the limitations in this study. We have been able to focus only on gestational alcohol consumption, although the effects of parental alcohol consumption on gametes prior to fertilization can also affect embryonic development [114, 115]. Also, the effects of common concurrent factors such as smoking,

antidepressants, and other drugs and their interactions, cannot be completely excluded. Although we managed to separate PAE-specific alterations, the confounding effect of smoking can be seen in both DNAm and mRNA-seq analyses. The high number of placentas exposed to both alcohol and smoking (82.5%) as well as potential interaction of these two or other potential factors may explain the smaller effect size of PAE than was expected. Notably, when PAE-associated genes were compared to a meta-analysis of placental DNAm changes associated with maternal smoking [116], nine common genes were found. However, seven of these genes were detected also in the sensitivity analyses of the non-smoking samples, and according to this, only *INPP5A* and *MGRN1* associated with smoking in the current study. Finally, we need to consider that the amount and the timing of consumed alcohol is mainly self-reported by the mothers in a special outpatient clinic for pregnant women with substance use problems, and inaccuracy in this personal evaluation can occur [117]. Due to these limitations, in vitro experiments are a necessary part of this study.

Conclusions

By using the unique biological samples of PAE newborns as well as alcohol-exposed both hESCs and differentiated hESCs, our study shows the early effects of alcohol exposure on both embryonic and extraembryonic cells reveal interesting new candidate genes *DPPA4*, *FOXP2*, and *TACR3* for the effects of PAE as well as brings forth potential biomarkers for PAE or even FASD. The discovery of *DPPA4* and *FOXP2* introduces the role of chromatin modifiers in alcohol-induced developmental disorders in human. Inaccurate timing and efficiency of transcriptional programming due to unfavorable epigenetic environment could explain the wide spectrum of disorders in the FASD phenotype.

Abbreviations

Ad: Alcohol units consumed per week; ADHD: Attention deficit hyperactivity disorder; ASD: Autism spectrum disorder; AUDIT: Alcohol Use Disorders Identification Test; BEC: Buccal epithelial cells; BP: Biological process; ChIP: Chromatin immunoprecipitation; CS: Caesarian section; DKK1: Dickkopf1; DMP: Differentially methylated position; DMR: Differentially methylated region; DNAm: DNA methylation; DPPA2: Developmental pluripotency associated factor 2; DPPA4: Developmental pluripotency associated factor 4; ENCODE: Encyclopedia of DNA Elements; epiFASD: Epigenetics of FASD; FASD: Fetal alcohol spectrum disorder; FDR: False discovery rate; FOXP2: Transcription factor forkhead box P2; FuGu: Biomedicum Functional Genomics Unit; GO: Gene Ontology; GW: Gestational week; GWAM: Genome-wide average DNA methylation; HC: Head circumference; hESC: Human embryonic stem cell; IL: Induction of labor; MAF: Minor allele frequency; mCpH: Methylated non-CpG site; mRNA-seq: 3'mRNA sequencing; N_shelf: North shelf; N_shore: North shore; PAE: Prenatal alcohol exposure; PCA: Principal component analysis; qPCR: Quantitative PCR; Q-Q: Quantile-Quantile; S_shelf: South shelf; S_shore: South shore; SD: Standard deviation; SVD: Singular value decomposition; TACR3: Tachykinin Receptor 3; TBC1D5: TBC1 domain family member 5; TSS1500: 1500 bp upstream of transcription start site; TSS200: 200 bp upstream of transcription start site; UCSC: University of California, Santa Cruz; UTR: Untranslated region; WBC: White blood cell.

Supplementary Information

The online version contains supplementary material available at <https://doi.org/10.1186/s12916-022-02699-1>.

Additional file 1: Table S1. General information about PAE samples. **Table S2.** General information about control samples. **Table S3.** General characteristics of PAE, early PAE and control newborns as well as their mothers included in the genome-wide DNAm and mRNA-seq analyses. **Table S4.** Primers for EpiTYPER and ChIP-qPCR. **Table S5.** PCR protocols for EpiTYPER and ChIP-qPCR. **Table S6.** Antibodies for ChIP. **Table S7.** PAE-associated differentially methylated CpGs in the placenta analyzed by microarrays. **Table S8.** PAE-associated differentially methylated CpGs in the placenta: sensitivity analysis for DMPs. **Table S9.** PAE-associated differentially methylated CpGs in the placenta: sensitivity analysis for candidate genes. **Table S10.** PAE-associated DMRs in the placenta. **Table S11.** Early PAE-associated differentially methylated CpGs in the placenta. **Table S12.** Early PAE-associated differentially methylated CpGs in the placenta: sensitivity analysis for DMPs. **Table S13.** Early PAE-associated differentially methylated CpGs in the placenta: sensitivity analysis for candidate genes. **Table S14.** Early PAE-associated DMRs in the placenta. **Table S15.** PAE-associated differentially methylated CpGs in the placenta: adjusted by cell type. **Table S16.** PAE-associated DMRs in the placenta: adjusted by cell type. **Table S17.** Early PAE-associated differentially methylated CpGs in the placenta: adjusted by cell type. **Table S18.** Early PAE-associated DMRs in the placenta: adjusted by cell type. **Table S19.** Pathway analysis of placental DMPs. **Table S20.** Pathway analysis of placental DMRs. **Table S21.** Sample-specific normalized placental DNAm levels (analyzed by microarrays) of target genes selected for EpiTYPER analysis. **Table S22.** PAE-associated differentially expressed genes in the placenta analyzed by mRNA-seq. **Table S23.** Pathway analysis of differentially expressed genes in PAE placentas. **Table S24.** Early PAE-associated differentially expressed genes in the placenta. **Table S25.** Genes with significant PAE-associated correlation between placental DNAm and mRNA expression. **Table S26.** Alcohol-induced differentially methylated CpGs and mCpGs in hESCs analyzed by microarrays. **Table S27.** Alcohol-induced DMRs in hESCs. **Table S28.** Pathway analysis of DMPs in hESCs. **Table S29.** Pathway analysis of DMRs in hESCs. **Table S30.** Differentially expressed genes in alcohol-exposed hESCs analyzed by mRNA-seq. **Table S31.** Pathway analysis of differentially expressed genes in hESCs. **Table S32.** Genes with significant alcohol exposure-associated correlation between DNAm and mRNA expression in hESCs. **Table S33.** DNAm levels of *DPPA4* regulatory region in alcohol-exposed and control hESCs analyzed by EpiTYPER. **Table S34.** Common alcohol exposure-associated genes in genome-wide DNAm and mRNA-seq analyses of placenta and hESCs. **Table S35.** Pathway analysis of common genes associated significantly with alcohol exposure in genome-wide DNAm analyses of placenta and hESCs. **Table S36.** Common genes in genome-wide DNAm analyses of placenta and hESCs previously associated with alcohol exposure. **Table S37.** Common genes and DMPs in genome-wide DNAm analysis of placenta previously associated with alcohol exposure in BECs of FASD or PAE children.

Additional file 2: Figure S1. Timing and amount of maternal alcohol consumption in categories **Figure S2.** Characterization of hESC differentiation into germ layer cells **Figure S3.** Q-Q plots of genome-wide DNAm (adjusted by smoking and sex) and sensitivity analyses (adjusted by sex, maternal age, mode of delivery, and parity) **Figure S4.** SVD plots of sensitivity analysis for candidate genes **Figure S5.** PCA for PAE-associated DMPs in placenta **Figure S6.** Effect sizes of candidate gene DMPs in genome-wide DNAm and sensitivity analyses **Figure S7.** Schematic figure about PAE-associated DMR at *IGF2/H19* locus in placenta **Figure S8.** Cell-type composition in placental samples **Figure S9.** GWAM comparison between control and PAE placentas **Figure S10.** GWAM comparison between alcohol-exposed and control hESCs **Figure S11.** Pathway analysis of DMPs in hESCs **Figure S12.** Pathway analysis of DMRs in hESCs **Figure S13.** Pathway analysis of differentially expressed genes in hESCs.

Acknowledgements

We are grateful to all the families who took part in this study. We would also like to acknowledge research nurse Teija Karkkulainen for her contribution to

this work, Dr Sailalitha Bollepalli for her bioinformatic assistance, and Adjunct Professor Keijo Viiri for his guidance in ChIP.

Authors' contributions

P.A., J.V., T.O., H.S., M.O., T.R., and N.K-A. contributed to the study design. H.K. recruited the study participants. P.A., J.V., H.M., E.W., L.A., and N.K-A. contributed to the sample collection and processing. P.A., J.S., E.W., K.R., and N.K-A. contributed to the laboratory experiments. P.A., J.V., H.M., M.V., A.S., M.O., and N.K-A. contributed to the data analysis. P.A. and N.K-A. drafted the manuscript. All authors contributed to the revision of the manuscript. All authors gave final approval of the version to be published.

Funding

This project was supported by the Academy of Finland (332212), University of Helsinki (Early Career Investigator Funding, Faculty of Medicine), Finnish Foundation for Alcohol Studies, Yrjö Jahansson Foundation, Juha Vainio Foundation, and Paulo Foundation (N.K-A.), Finnish Cultural Foundation (00190186, 00200185, and 00212573) (P.A.), Finnish Foundation for Alcohol Studies (H.M.), Estonian Research Council (PRG1076), Horizon 2020 innovation (ERIN, EU952516) and European Commission and Enterprise Estonia (EU48695) (A.S.), Jane and Aatos Erkkö Foundation, Academy of Finland (297466, 312437), and Center of Excellence in Stem Cell Metabolism (T.O.), Academy of Finland (297886) (H.S.), Academy of Finland (297908 and 328685) and Sigrid Jusélius Foundation (M.O.), and Sigrid Jusélius Foundation (R.T.)

Availability of data and materials

The datasets supporting the conclusions of the current study are included within the article and its additional files. Due to the sensitive nature of the patient data used, the data sets are not and cannot be made publicly available. The other data that support the findings of this study, such as the codes, is available from the corresponding author, NKA, upon reasonable request.

Declarations

Ethics approval and consent to participate

Informed consent was obtained from all participants and the study was approved by the Ethics Committee of Helsinki University Central Hospital (386/13/03/03/2012). hESC cell line H1 (WA01) was obtained from Biomedicum Stem Cell Center (BSCC, Helsinki, Finland) through a license agreement with WiCell, Inc. and Regea08/017 from Skottman laboratory (Tampere, Finland) approved by the Ethics Committee of Tampere University Hospital (Skottman/R05116).

Competing interests

The authors declare that they have no competing interests.

Author details

¹Environmental Epigenetics Laboratory, Department of Medical and Clinical Genetics, Medicum, University of Helsinki, 00290 Helsinki, Finland. ²Department of Obstetrics and Gynaecology, Institute of Clinical Medicine, University of Tartu, 50406 Tartu, Estonia. ³Competence Centre on Health Technologies, 50411 Tartu, Estonia. ⁴Research Programs Unit, Stem cells and Metabolism and Biomedicum Stem Cell Centre, Faculty of Medicine, University of Helsinki, 00014 Helsinki, Finland. ⁵Division of Obstetrics and Gynaecology, Department of Clinical Science, Intervention and Technology (CLINTEC), Karolinska Institutet, S-171 76 Stockholm, Sweden. ⁶Children's Hospital, Helsinki University Central Hospital, University of Helsinki, 00290 Helsinki, Finland. ⁷Faculty of Medicine and Health Technology, Tampere University, 33520 Tampere, Finland. ⁸Institute for Molecular Medicine, Finland, FIMM, HiLIFE, University of Helsinki, 00290 Helsinki, Finland. ⁹Obstetrics and Gynecology, Helsinki University Hospital, University of Helsinki, 00290 Helsinki, Finland.

Received: 25 July 2022 Accepted: 7 December 2022

Published online: 30 December 2022

References

- Hoyme HE, Kalberg WO, Elliott AJ, Blankenship J, Buckley D, Marais AS, et al. Updated clinical guidelines for diagnosing fetal alcohol spectrum disorders. *Pediatrics*. 2016;138:e20154256.
- Roozen S, Peters GJY, Kok G, Townend D, Nijhuis J, Curfs L. Worldwide prevalence of fetal alcohol spectrum disorders: a systematic literature review including meta-analysis (vol 40, pg 18, 2016). *Alcohol Clin Exp Res*. 2016;40(7):1587.
- Tobi EW, Sliker RC, Stein AD, Suchiman HE, Slagboom PE, van Zwet EW, et al. Early gestation as the critical time-window for changes in the prenatal environment to affect the adult human blood methylome. *Int J Epidemiol*. 2015;44:1211–23.
- Susiarjo M, Sasson I, Mesaros C, Bartolomei MS. Bisphenol A exposure disrupts genomic imprinting in the mouse. *PLoS Genet*. 2013;9:e1003401.
- Kaminen-Ahola N, Ahola A, Maga M, Mallitt KA, Fahey P, Cox TC, et al. Maternal ethanol consumption alters the epigenotype and the phenotype of offspring in a mouse model. *PLoS Genet*. 2010;6:e1000811.
- Zhang CR, Ho MF, Vega MCS, Burne THJ, Chong S. Prenatal ethanol exposure alters adult hippocampal VGLUT2 expression with concomitant changes in promoter DNA methylation, H3K4 trimethylation and miR-467b-5p levels. *Epigenetics Chromatin*. 2015;8:40.
- Khalid O, Kim JJ, Kim HS, Hoang M, Tu TG, Elie O, et al. Gene expression signatures affected by alcohol-induced DNA methylomic deregulation in human embryonic stem cells. *Stem Cell Res*. 2014;12:791–806.
- Sanchez-Alvarez R, Gayen S, Vadigepalli R, Anni H. Ethanol diverts early neuronal differentiation trajectory of embryonic stem cells by disrupting the balance of lineage specifiers. *PLoS One*. 2013;8:e63794.
- Zhu Y, Gomez JA, Laufer BI, Mordaunt CE, Mouat JS, Soto DC, et al. Placental methylome reveals a 22q13.33 brain regulatory gene locus associated with autism. *Genome Biol*. 2022;23:46.
- Laufer BI, Neier K, Valenzuela AE, Yasui DH, Schmidt RJ, Lein PJ, et al. Placenta and fetal brain share a neurodevelopmental disorder DNA methylation profile in a mouse model of prenatal PCB exposure. *Cell Rep*. 2022;38:110442.
- Hernandez C, Wang Z, Ramazanov B, Tang Y, Mehta S, Dambrot C, et al. Dppa2/4 facilitate epigenetic remodeling during reprogramming to pluripotency. *Cell Stem Cell*. 2018;23:396–411 e8.
- Eckersley-Maslin MA, Parry A, Blotenburg M, Krueger C, Ito Y, Franklin VNR, et al. Epigenetic priming by Dppa2 and 4 in pluripotency facilitates multi-lineage commitment. *Nat Struct Mol Biol*. 2020;27:696–705.
- Gretarsson KH, Hackett JA. Dppa2 and Dppa4 counteract de novo methylation to establish a permissive epigenome for development. *Nat Struct Mol Biol*. 2020;27:706–16.
- Eckersley-Maslin M, Alda-Catalinas C, Blotenburg M, Kreibich E, Krueger C, Reik W. Dppa2 and Dppa4 directly regulate the dux-driven zygotic transcriptional program. *Genes Dev*. 2019;33:194–208.
- Cobben JM, Krzyzewska IM, Venema A, Mul AN, Polstra A, Postma AV, et al. DNA methylation abundantly associates with fetal alcohol spectrum disorder and its subphenotypes. *Epigenomics*. 2019;11:767–85.
- Portales-Casamar E, Lussier AA, Jones MJ, Maclsaac JL, Edgar RD, Mah SM, et al. DNA methylation signature of human fetal alcohol spectrum disorder. *Epigenetics Chromatin*. 2016;9:25.
- Lussier AA, Morin AM, Maclsaac JL, Salmon J, Weinberg J, Reynolds JN, et al. DNA methylation as a predictor of fetal alcohol spectrum disorder. *Clin Epigenetics*. 2018;10:5.
- Babor TF, Higgins-Biddle JC, Saunders JB, Monteiro MG. AUDIT the alcohol use disorders identification test, guidelines for use in primary care: World Health Organization; 2001.
- Rehm J, Gmel G, Probst C, Shield KD. Lifetime-risk of alcohol-attributable mortality based on different levels of alcohol consumption in seven European countries. Implications for low-risk drinking guidelines. Toronto: Centre for Addiction and Mental Health; 2015.
- Tynjala J, Kangastupa P, Laatikainen T, Aalto M, Niemela O. Effect of age and gender on the relationship between alcohol consumption and serum GGT: time to recalibrate goals for normal ranges. *Alcohol Alcohol*. 2012;47:558–62.
- Marjonen H, Auvinen P, Kahila H, Tsuiho O, Koks S, Tiirats A, et al. rs10732516 polymorphism at the IGF2/H19 locus associates with genotype-specific effects on placental DNA methylation and birth weight of newborns conceived by assisted reproductive technology. *Clin Epigenetics*. 2018;10:80.
- PediTools. <http://peditools.org>. Accessed 24 Oct 2022.
- Fenton TR, Nasser R, Eliasziw M, Kim JH, Bilan D, Sauve R. Validating the weight gain of preterm infants between the reference growth curve of the fetus and the term infant. *BMC Pediatr*. 2013;13:92.
- Dolganiuc A, Szabo G. In vitro and in vivo models of acute alcohol exposure. *World J Gastroenterol*. 2009;15:1168–77.
- De Filippis L, Halikere A, McGowan H, Moore JC, Tischfield JA, Hart RP, et al. Ethanol-mediated activation of the NLRP3 inflammasome in iPS cells and iPS cells-derived neural progenitor cells. *Mol Brain*. 2016;9:51.
- Tian Y, Morris TJ, Webster AP, Yang Z, Beck S, Feber A, et al. ChAMP: updated methylation analysis pipeline for Illumina BeadChips. *Bioinformatics*. 2017;33:3982–4.
- McCartney DL, Walker RM, Morris SW, McIntosh AM, Porteous DJ, Evans KL. Identification of polymorphic and off-target probe binding sites on the Illumina Infinium MethylationEPIC BeadChip. *Genom Data*. 2016;9:22–4.
- Gupta R, van Dongen J, Fu Y, Abdellaoui A, Tyndale RF, Velagapudi V, et al. Epigenome-wide association study of serum cotinine in current smokers reveals novel genetically driven loci. *Clin Epigenetics*. 2019;11:1.
- Zhou W, Laird PW, Shen H. Comprehensive characterization, annotation and innovative use of Infinium DNA methylation BeadChip probes. *Nucleic Acids Res*. 2017;45:e22.
- Johnson WE, Li C, Rabinovic A. Adjusting batch effects in microarray expression data using empirical Bayes methods. *Biostatistics*. 2007;8:118–27.
- Ritchie ME, Phipson B, Wu D, Hu Y, Law CW, Shi W, et al. Limma powers differential expression analyses for RNA-sequencing and microarray studies. *Nucleic Acids Res*. 2015;43:e47.
- Yuan V, Hui D, Yin Y, Penaherrera MS, Beristain AG, Robinson WP. Cell-specific characterization of the placental methylome. *BMC Genomics*. 2021;22:6.
- Gilad lab. <http://giladlab.uchicago.edu>. Accessed 24 Oct 2022.
- Hansen K. IlluminaHumanMethylationEPICanno.ilm10b4.hg19: Annotation for Illumina's EPIC methylation arrays. R package version 0.6.0. 2017. https://bitbucket.com/kasperdanielhansen/Illumina_EPIC. Accessed 24 Oct 2022.
- Illumina. <https://www.illumina.com>. Accessed 24 Oct 2022.
- Kolde R, Martens K, Løkk K, Laur S, Vilo J. SeqM: an MDL based method for identifying differentially methylated regions in high density methylation array data. *Bioinformatics*. 2016;32:2604–10.
- Li S, Wong EM, Dugue PA, McRae AF, Kim E, Joo JHE, et al. Genome-wide average DNA methylation is determined in utero. *Int J Epidemiol*. 2018;47:908–16.
- Zheng Y, Joyce BT, Liu L, Zhang Z, Kibbe WA, Zhang W, et al. Prediction of genome-wide DNA methylation in repetitive elements. *Nucleic Acids Res*. 2017;45:8697–711.
- Phipson B, Maksimovic J, Oshlack A. missMethyl: an R package for analyzing data from Illumina's HumanMethylation450 platform. *Bioinformatics*. 2016;32:286–8.
- Agena Bioscience I. EpiDesigner. <http://www.epidesigner.com>. Accessed 24 Oct 2022.
- Macosko EZ, Basu A, Satija R, Nemes J, Shekhar K, Goldman M, et al. Highly parallel genome-wide expression profiling of individual cells using nanoliter droplets. *Cell*. 2015;161:1202–14.
- Love MI, Huber W, Anders S. Moderated estimation of fold change and dispersion for RNA-seq data with DESeq2. *Genome Biol*. 2014;15:550.
- Zhang Y, Parmigiani G, Johnson WE. ComBat-seq: batch effect adjustment for RNA-seq count data. *NAR Genom Bioinform*. 2020;2:lqaa078.
- Wu T, Hu E, Xu S, Chen M, Guo P, Dai Z, et al. clusterProfiler 4.0: a universal enrichment tool for interpreting omics data. *Innovation (N Y)*. 2021;2:100141.
- Cedoz PL, Prunello M, Brennan K, Gevaert O. MethylMix 2.0: an R package for identifying DNA methylation genes. *Bioinformatics*. 2018;34:3044–6.
- Schmidt D, Wilson MD, Spyrou C, Brown GD, Hadfield J, Odom DT. ChIP-seq: using high-throughput sequencing to discover protein-DNA interactions. *Methods*. 2009;48:240–8.
- ENCODE. <https://encodeproject.org>. Accessed 24 Oct 2022.
- Rozen S, Skaletsky H. Primer3 on the WWW for general users and for biologist programmers. *Methods Mol Biol*. 2000;132:365–86.

49. di Pietro M, Lao-Sirieix P, Boyle S, Cassidy A, Castillo D, Saadi A, et al. Evidence for a functional role of epigenetically regulated midcluster HOXB genes in the development of Barrett esophagus. *Proc Natl Acad Sci U S A*. 2012;109:9077–82.
50. R Core Team. R: a language and environment for statistical computing. Vienna: R Foundation for Statistical Computing; 2022. <https://www.R-project.org>
51. Elliott-Sale KJ, Graham A, Hanley SJ, Blumenthal S, Sale C. Modern dietary guidelines for healthy pregnancy; maximising maternal and foetal outcomes and limiting excessive gestational weight gain. *Eur J Sport Sci*. 2019;19:62–70.
52. Vernes SC, Oliver PL, Spiteri E, Lockstone HE, Puliyadi R, Taylor JM, et al. Foxp2 regulates gene networks implicated in neurite outgrowth in the developing brain. *PLoS Genet*. 2011;7:e1002145.
53. Lai CSL, Fisher SE, Hurst JA, Vargha-Khadem F, Monaco AP. A forkhead-domain gene is mutated in a severe speech and language disorder. *Nature*. 2001;413:519–23.
54. Foroud T, Wetherill LF, Kramer J, Tischfield JA, Nurnberger JI, Schuckit MA, et al. The tachykinin receptor 3 is associated with alcohol and cocaine dependence. *Alcohol Clin Exp Res*. 2008;32:1023–30.
55. Barros M, Dempster EL, Illott N, Chabrawi S, Maior RS, Tomaz C, et al. Decreased methylation of the NK3 receptor coding gene (TACR3) after cocaine-induced place preference in marmoset monkeys. *Addict Biol*. 2013;18:452–4.
56. Alberry BLJ, Singh SM. Hippocampal DNA methylation in a mouse model of fetal alcohol spectrum disorder that includes maternal separation stress only partially explains changes in gene expression. *Front Genet*. 2020;11:70.
57. Lussier AA, Bodnar TS, Moksa M, Hirst M, Kobor MS, Weinberg J. Prenatal adversity alters the epigenetic profile of the prefrontal cortex: sexually dimorphic effects of prenatal alcohol exposure and food-related stress. *Genes (Basel)*. 2021;12:1773.
58. Carter RC, Chen J, Li Q, Deyssenroth M, Dodge NC, Wainwright HC, et al. Alcohol-related alterations in placental imprinted gene expression in humans mediate effects of prenatal alcohol exposure on postnatal growth. *Alcohol Clin Exp Res*. 2018. <https://doi.org/10.1111/acer.13808>.
59. Laufer BI, Mantha K, Kleiber ML, Diehl EJ, Addison SM, Singh SM. Long-lasting alterations to DNA methylation and ncRNAs could underlie the effects of fetal alcohol exposure in mice. *Dis Model Mech*. 2013;6:977–92.
60. Haycock PC, Ramsay M. Exposure of mouse embryos to ethanol during preimplantation development: effect on DNA methylation in the h19 imprinting control region. *Biol Reprod*. 2009;81(4):618–27.
61. Marjonen H, Kahila H, Kaminen-Ahola N. rs10732516 polymorphism at the IGF2/H19 locus associates with a genotype-specific trend in placental DNA methylation and head circumference of prenatally alcohol-exposed newborns. *Hum Reprod Open*. 2017;2017:hox014.
62. Sharp GC, Arathimos R, Reese SE, Page CM, Felix J, Kupers LK, et al. Maternal alcohol consumption and offspring DNA methylation: findings from six general population-based birth cohorts. *Epigenomics*. 2018;10:27–42.
63. Yuen RKC, Merico D, Bookman M, Howe JL, Thiruvahindrapuram B, Patel RV, et al. Whole genome sequencing resource identifies 18 new candidate genes for autism spectrum disorder. *Nat Neurosci*. 2017;20:602–11.
64. Bill BR, Lowe JK, Dybuncio CT, Fogel BL. Orchestration of neurodevelopmental programs by RFX1: implications for autism spectrum disorder. *Int Rev Neurobiol*. 2013;113:251–67.
65. Tai M, Piskorski A, Kao JC, Hess LA, MdIM S, Gundogan F. Placental morphology in fetal alcohol spectrum disorders. *Alcohol Alcohol*. 2017;52:138–44.
66. Lander ES, Linton LM, Birren B, Nussbaum C, Zody MC, Baldwin J, et al. Initial sequencing and analysis of the human genome. *Nature*. 2001;409:860–921.
67. Chung YM, Kim JS, Yoo YD. A novel protein, Romo1, induces ROS production in the mitochondria. *Biochem Biophys Res Commun*. 2006;347:649–55.
68. Mu ZM, Yin XY, Prochownik EV. Pag, a putative tumor suppressor, interacts with the Myc box II domain of c-Myc and selectively alters its biological function and target gene expression. *J Biol Chem*. 2002;277:43175–84.
69. Semenza GL. Regulation of oxygen homeostasis by hypoxia-inducible factor 1. *Birth Defects Res A*. 2008;82:314.
70. Chu J, Tong M, de la Monte SM. Chronic ethanol exposure causes mitochondrial dysfunction and oxidative stress in immature central nervous system neurons. *Acta Neuropathol*. 2007;113:659–73.
71. Chen JJ, Schenker S, Henderson GI. 4-hydroxynonenol levels are enhanced in fetal liver mitochondria by in utero ethanol exposure. *Hepatology*. 1997;25:142–7.
72. Gundogan F, Elwood G, Mark P, Feijoo A, Longato L, Tong M, et al. Ethanol-induced oxidative stress and mitochondrial dysfunction in rat placenta: relevance to pregnancy loss. *Alcohol Clin Exp Res*. 2010;34:415–23.
73. Holland O, Dekker Nitert M, Gallo LA, Vejzovic M, Fisher JJ, Perkins AV. Review: placental mitochondrial function and structure in gestational disorders. *Placenta*. 2017;54:2–9.
74. Ahamed M, Mehrotra PK, Kumar P, Siddiqui MK. Placental lead-induced oxidative stress and preterm delivery. *Environ Toxicol Pharmacol*. 2009;27:70–4.
75. Marvin MJ, Di Rocco G, Gardiner A, Bush SM, Lassar AB. Inhibition of Wnt activity induces heart formation from posterior mesoderm. *Genes Dev*. 2001;15:316–27.
76. Mukhopadhyay M, Shtrom S, Rodriguez-Esteban C, Chen L, Tsukui T, Gomer L, et al. Dickkopf1 is required for embryonic head induction and limb morphogenesis in the mouse. *Dev Cell*. 2001;1:423–34.
77. Fedi P, Bañico A, Nieto Soria A, Burgess WH, Miki T, Bottaro DP, et al. Isolation and biochemical characterization of the human Dkk-1 homologue, a novel inhibitor of mammalian Wnt signaling. *J Biol Chem*. 1999;274:19465–72.
78. Zhang Z, Wang X, Zhang L, Shi Y, Wang J, Yan H. Wnt/beta-catenin signaling pathway in trophoblasts and abnormal activation in preeclampsia (review). *Mol Med Rep*. 2017;16:1007–13.
79. Zhang L, Leng M, Li Y, Yuan Y, Yang B, Li Y, et al. Altered DNA methylation and transcription of WNT2 and DKK1 genes in placentas associated with early-onset preeclampsia. *Clin Chim Acta*. 2019;490:154–60.
80. Zhang Z, Li H, Zhang L, Jia L, Wang P. Differential expression of beta-catenin and Dickkopf-1 in the third trimester placentas from normal and preeclamptic pregnancies: a comparative study. *Reprod Biol Endocrinol*. 2013;11:17.
81. Bao SH, Shuai W, Tong J, Wang L, Chen P, Duan T. Increased Dickkopf-1 expression in patients with unexplained recurrent spontaneous miscarriage. *Clin Exp Immunol*. 2013;172:437–43.
82. Thomson M, Liu SJ, Zou LN, Smith Z, Meissner A, Ramanathan S. Pluripotency factors in embryonic stem cells regulate differentiation into germ layers. *Cell*. 2011;145:875–89.
83. Jimenez-Organ A, Kvainickas A, Nagele H, Denner J, Eimer S, Dengjel J, et al. Control of RAB7 activity and localization through the retromer-TBC1D5 complex enables RAB7-dependent mitophagy. *EMBO J*. 2018;37:235–54.
84. Yang L, Yang C, Thomes PG, Kharbanda KK, Casey CA, McNiven MA, et al. Lipophagy and alcohol-induced fatty liver. *Front Pharmacol*. 2019;10:495.
85. Lin H, Guo X, Liu J, Liu P, Mei G, Li H, et al. Improving lipophagy by restoring Rab7 cycle: protective effects of quercetin on ethanol-induced liver steatosis. *Nutrients*. 2022;14:658.
86. Elia J, Gai X, Xie HM, Perin JC, Geiger E, Glessner JT, et al. Rare structural variants found in attention-deficit hyperactivity disorder are preferentially associated with neurodevelopmental genes. *Mol Psychiatry*. 2010;15:637–46.
87. Liu X, Xie H, Fu Z, Yao Q, Han T, Zhan D, et al. MAD1L1 and TSNARE gene polymorphisms are associated with schizophrenia susceptibility in the Han Chinese population. *BMC Med Genet*. 2021;14:218.
88. Shi J, Levinson DF, Duan J, Sanders AR, Zheng Y, Pe'er I, et al. Common variants on chromosome 6p22.1 are associated with schizophrenia. *Nature*. 2009;460:753–7.
89. Frey S, Eichler A, Stonawski V, Kriebel J, Wahl S, Gallati S, et al. Prenatal alcohol exposure is associated with adverse cognitive effects and distinct whole-genome DNA methylation patterns in primary school children. *Front Behav Neurosci*. 2018;12:125.

90. Kietzman HW, Everson JL, Sulik KK, Lipinski RJ. The teratogenic effects of prenatal ethanol exposure are exacerbated by sonic hedgehog or *Gli2* haploinsufficiency in the mouse. *PLoS One*. 2014;9:e89448.
91. Masaki H, Nishida T, Kitajima S, Asahina K, Teraoka H. Developmental pluripotency-associated 4 (DPPA4) localized in active chromatin inhibits mouse embryonic stem cell differentiation into a primitive ectoderm lineage. *J Biol Chem*. 2007;282:33034–42.
92. Wang Z, Oron E, Nelson B, Razis S, Ivanova N. Distinct lineage specification roles for NANOG, OCT4, and SOX2 in human embryonic stem cells. *Cell Stem Cell*. 2012;10:440–54.
93. Ying L, Mills JA, French DL, Gadue P. OCT4 coordinates with WNT signaling to pre-pattern chromatin at the SOX17 locus during human ES cell differentiation into definitive endoderm. *Stem Cell Reports*. 2015;5:490–8.
94. Hickey SL, Berto S, Konopka G. Chromatin decondensation by FOXP2 promotes human neuron maturation and expression of neurodevelopmental disease genes. *Cell Rep*. 2019;27:1699–1711.e9.
95. Vargha-Khadem F, Watkins K, Alcock K, Fletcher P, Passingham R. Praxic and nonverbal cognitive deficits in a large family with a genetically transmitted speech and language disorder. *Proc Natl Acad Sci U S A*. 1995;92:930–3.
96. Watkins KE, Vargha-Khadem F, Ashburner J, Passingham RE, Connelly A, Friston KJ, et al. MRI analysis of an inherited speech and language disorder: structural brain abnormalities. *Brain*. 2002;125:465–78.
97. Demontis D, Walters RK, Martin J, Mattheisen M, Als TD, Agerbo E, et al. Discovery of the first genome-wide significant risk loci for attention deficit/hyperactivity disorder. *Nat Genet*. 2019;51:63–75.
98. Lange S, Rehm J, Anagnostou E, Popova S. Prevalence of externalizing disorders and autism spectrum disorders among children with fetal alcohol spectrum disorder: systematic review and meta-analysis. *Biochem Cell Biol*. 2018;96:241–51.
99. Popova S, Lange S, Shield K, Mihic A, Chudley AE, Mukherjee RAS, et al. Comorbidity of fetal alcohol spectrum disorder: a systematic review and meta-analysis. *Lancet*. 2016;387:978–87.
100. O’Roak BJ, Deriziotis P, Lee C, Vives L, Schwartz JJ, Girirajan S, et al. Exome sequencing in sporadic autism spectrum disorders identifies severe de novo mutations. *Nat Genet*. 2011;43:585–9.
101. Mukamel Z, Konopka G, Wexler E, Osborn GE, Dong HM, Bergman MY, et al. Regulation of MET by FOXP2, genes implicated in higher cognitive dysfunction and autism risk. *J Neurosci*. 2011;31:11437–42.
102. Choi L, An JY. Genetic architecture of autism spectrum disorder: lessons from large-scale genomic studies. *Neurosci Biobehav Rev*. 2021;128:244–57.
103. Stevens SA, Nash K, Koren G, Rovet J. Autism characteristics in children with fetal alcohol spectrum disorders. *Child Neuropsychol*. 2013;19:579–87.
104. Laufer BI, Kapalanga J, Castellani CA, Diehl EJ, Yan L, Singh SM. Associative DNA methylation changes in children with prenatal alcohol exposure. *Epigenomics*. 2015;7:1259–74.
105. Zhang WW, Wang Y, Chu YX. *Tacr3/NK3R*: beyond their roles in reproduction. *ACS Chem Neurosci*. 2020;11:2935–43.
106. de Souza Silva MA, Lenz B, Rotter A, Biermann T, Peters O, Ramirez A, et al. Neurokinin3 receptor as a target to predict and improve learning and memory in the aged organism. *Proc Natl Acad Sci U S A*. 2013;110:15097–102.
107. Loke YJ, Muggli E, Saffery R, Ryan J, Lewis S, Elliott EJ, et al. Sex- and tissue-specific effects of binge-level prenatal alcohol consumption on DNA methylation at birth. *Epigenomics*. 2021;13:1921–38.
108. Treit S, Chen Z, Zhou D, Baugh L, Rasmussen C, Andrew G, et al. Sexual dimorphism of volume reduction but not cognitive deficit in fetal alcohol spectrum disorders: a combined diffusion tensor imaging, cortical thickness and brain volume study. *Neuroimage Clin*. 2017;15:284–97.
109. Loke YJ, Muggli E, Nguyen L, Ryan J, Saffery R, Elliott EJ, et al. Time- and sex-dependent associations between prenatal alcohol exposure. *Epigenomics*. 2018;10:981–91.
110. Kaminen-Ahola N. Fetal alcohol spectrum disorders: genetic and epigenetic mechanisms. *Prenat Diagn*. 2020;40:1185–92.
111. Armant DR, Saunders DE. Exposure of embryonic cells to alcohol: contrasting effects during preimplantation and postimplantation development. *Semin Perinatol*. 1996;20:127–39.
112. Organization WH. Global status report on alcohol and health 2018. Geneva: World Health Organization; 2018.
113. Bearak J, Popinchalk A, Alkema L, Sedgh G. Global, regional, and sub-regional trends in unintended pregnancy and its outcomes from 1990 to 2014: estimates from a Bayesian hierarchical model. *Lancet Glob Health*. 2018;6:e380–e9.
114. Bielawski DM, Abel EL. Acute treatment of paternal alcohol exposure produces malformations in offspring. *Alcohol*. 1997;14:397–401.
115. Chang RC, Wang H, Bedi Y, Golding MC. Preconception paternal alcohol exposure exerts sex-specific effects on offspring growth and long-term metabolic programming. *Epigenetics Chromatin*. 2019;12:9.
116. Everson TM, Vives-Usano M, Seyve E, Cardenas A, Lacasana M, Craig JM, et al. Placental DNA methylation signatures of maternal smoking during pregnancy and potential impacts on fetal growth. *Nat Commun*. 2021;12:5095.
117. Lange S, Shield K, Koren G, Rehm J, Popova S. A comparison of the prevalence of prenatal alcohol exposure obtained via maternal self-reports versus meconium testing: a systematic literature review and meta-analysis. *BMC Pregnancy Childbirth*. 2014;14:127.

Publisher’s Note

Springer Nature remains neutral with regard to jurisdictional claims in published maps and institutional affiliations.

Ready to submit your research? Choose BMC and benefit from:

- fast, convenient online submission
- thorough peer review by experienced researchers in your field
- rapid publication on acceptance
- support for research data, including large and complex data types
- gold Open Access which fosters wider collaboration and increased citations
- maximum visibility for your research: over 100M website views per year

At BMC, research is always in progress.

Learn more biomedcentral.com/submissions

